Supplementary Information (SI) for ChemComm.

Table of Content

1. Materials and Methods

Reagents and solvents were purchased as reagent grade and were used without further purification. Column chromatography was carried out on silica gel (200–300 mesh). IR spectra were recorded on a Thermo Scientific Nicolet Summit LITI FTIR spectrometer (Everest ATR) and are reported as wavenumbers ν in cm^{-1} with band intensities indicated as s (strong), m (medium), w (weak). ^{1}H and ^{13}C spectra were recorded (as indicated) on a Bruker 400 MHz spectrometer and are reported as chemical shifts (δ) in ppm relative to residual signals of the solvents ($CDCl_3$: 7.26 ppm; $SO(CD_3)_2$: 2.50 ppm). ^{13}C NMR chemical shifts were reported in ppm relative to the solvent ($CDCl_3$: 77.16 ppm; $SO(CD_3)_2$: 39.92 ppm). Spin multiplicities are reported as a singlet (s), doublet (d), triplet (t) and quartet (q), with coupling constants (J) given in Hz, or multiplet (m). Broad peaks are marked as br. High resolution mass spectrometry (HRMS) was obtained on a Q-TOF micro spectrometer. Melting points were determined with an auto melting point system.

Abbreviations. DCM: dichloromethane; EDCI: 1-ethyl-3(3-dimethylpropylamine) carbodiimide; DMAP: 4-dimethylaminopyridine; HOBt: 1-hydroxybenzotriazole; EtOAc: ethyl acetate; PE: petroleum ether; DMSO: dimethyl sulfoxide; THF: tetrahydrofuran; MeOH: methanol; $TBANO_3$: tetrabutyl ammonium nitrate; rt: room temperature; eq: equivalent; mp: melting point; NMR: nuclear magnetic resonance

2. Synthesis

Compound 2 was synthesized as described in ref. S1.

Compound 3 was synthesized as described in ref. S2.

Compound 4 was synthesized as described in ref. S1.

Compound 8 was synthesized as described in ref. S3.

Compound 15 was synthesized as described in ref. S4.

Compounds 16, **19**, **20**, **22**, **23** and **25** are commercially available.

Compound 1, **9** and **11** were synthesized following a modified literature procedure (Scheme S1).[S1] To a solution of aryl acid **S1** (5.0 mmol) in DCM (40 mL) was added EDCI (1.0 g, 5.3 mmol) and DMAP (61.1 mg, 1.0 mmol) at rt, followed by the addition of **S2** (445.7 mg, 5.0 mmol) or **S3** (297.9 mg, 2.5 mmol). The reaction mixture was stirred at this temperature overnight. The resulting mixture was extracted with DCM (100 mL × 3). The combined organic layers were washed with saturated $NaHCO_3$ (50 mL) and brine (50 mL), dried over Na_2SO_4 and concentrated *in vacuo* to give the crude product. Silica gel column chromatography of the residue (DCM/MeOH 98:2) gave pure **1**, **9** and **11**.

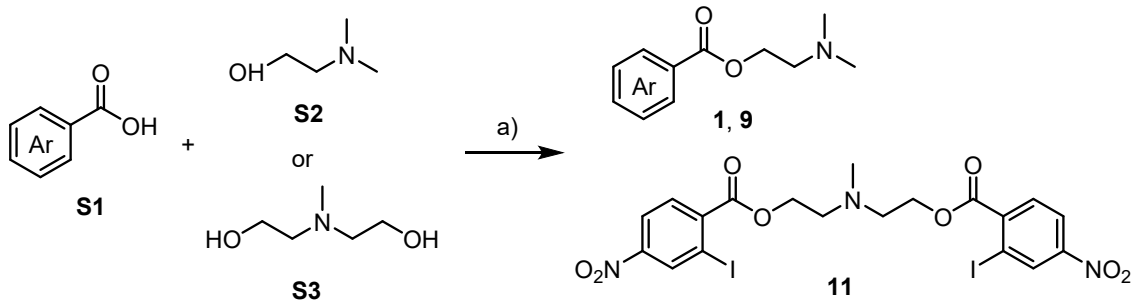

Scheme S1. (a) EDCI, DMAP, DCM, rt, overnight

Compound 1 was obtained as a pale-yellow oil, 1.4 g, 91%. IR (neat): 3099 (w), 2952 (w), 2825 (w), 2869 (w), 2775 (w), 2359 (w), 1731 (s), 1631 (w), 1546 (s), 1465 (m), 1358 (w), 1325 (s), 1260 (s), 1245 (s), 1177 (m), 1137 (s), 1104 (m), 1041 (w), 1007 (w), 979 (w), 916 (w), 886 (m), 773 (w), 740 (s), 725 (m), 688 (s); ^{1}H NMR (400 MHz, $CDCl_3$): 9.03 (t, *J* = 1.8 Hz, 1H), 8.69 – 8.63 (m, 1H), 8.61 – 8.60 (m, 1H), 4.51 (t, *J* = 5.8 Hz, 2H), 2.74 (t, *J* = 5.8 Hz, 2H), 2.33 (s, 6H); ^{13}C NMR (100 MHz, $CDCl_3$): 163.25, 148.47, 133.33, 132.80 (q, *J* = 34.8 Hz), 131.98 (q, *J* = 3.6 Hz), 127.59, 124.45 (q, *J* = 3.8 Hz), 122.42 (q, *J* = 273.2 Hz), 64.20, 57.67, 45.75; ^{19}F NMR (376 MHz, $CDCl_3$): -62.91. HRMS (ESI) calcd for $C_{12}H_{14}F_3N_2O_4$ $([M+H])^+$: 307.0900, found: 307.0903.

Compound 9 was obtained as a light yellow solid, 936.8 mg, 51%. Mp: 68 – 69 ^{o}C; IR (neat): 3096 (w), 2947 (w), 2823 (w), 2774 (w), 1731 (s), 1580 (w), 1524 (s), 1462 (m), 1345 (s), 1292 (s), 1245 (s), 1116 (m), 1031 (s), 956 (w), 896 (w), 842 (w), 780 (w), 731 (s); ^{1}H NMR (400 MHz, $CDCl_3$): 8.75 (d, *J* = 2.2 Hz, 1H), 8.21 (dd, *J* = 8.5, 2.2 Hz, 1H), 7.88 (d, *J* = 8.5 Hz, 1H), 4.46 (t, *J* = 5.8 Hz, 2H), 2.72 (t, *J* = 5.8 Hz, 2H), 2.31 (s, 6H); ^{13}C NMR (100 MHz, $CDCl_3$): 165.48, 148.87, 141.20, 135.77, 131.29, 122.82, 93.60, 77.48, 77.16, 76.84, 64.13, 57.58, 45.80; HRMS (ESI) calcd for $C_{11}H_{14}IN_2O_4$ $([M+H])^+$: 364.9993, found: 364.9994.

Compound 11 was obtained as a pale-brown solid, 1.3 g, 78%. Mp: 190 – 192 ^{o}C; IR (neat): 3263 (w), 3078 (w), 2951 (w), 1641 (s), 1546 (m), 1460 (w), 1383 (m), 1318 (s), 1259 (m), 1170 (s), 1127 (s), 1075 (s), 1044 (w), 893 (w), 840 (m), 791 (w), 737 (m), 698 (m), 640 (w); ^{1}H NMR (400 MHz, $CDCl_3$): 8.74 (d, *J* = 2.2 Hz, 2H), 8.17 (dd, *J* = 8.5, 2.2 Hz, 2H), 7.84 (d, *J* = 8.5 Hz, 2H), 4.49 (t, *J* = 5.8 Hz, 4H), 2.92 (t, *J* = 5.8 Hz, 4H), 2.46 (s, 3H); ^{13}C

NMR (100 MHz, $CDCl_3$): 165.38, 148.95, 141.01, 135.88, 131.27, 122.86, 93.59, 63.90, 56.00, 42.83; HRMS (ESI) calcd for $C_{19}H_{18}I_2N_3O_8$ ($[M+H]$)$^+$: 669.9178, found: 669.9177.

Compound 5-7, **10** and **12** were synthesized following a modified literature procedure (Scheme S2).[S2] To a solution of aryl acid **S1** (5.0 mmol) in DCM (40 mL) was added EDCI (1.0 g, 5.3 mmol) at rt, followed by the addition of **S4** (440.5 mg, 5.0 mmol) or **S5** (293.0 mg, 2.5 mmol) or **S6** (234.0 mg, 1.6 mmol). The reaction mixture was stirred at this temperature overnight. The resulting mixture was extracted with DCM (100 mL × 3). The combined organic layers were washed with saturated $NaHCO_3$ (50 mL) and brine (50 mL), dried over Na_2SO_4 and concentrated *in vacuo* to give the crude product. Silica gel column chromatography of the residue (DCM/MeOH 90:10) gave pure **5-7**, **10** and **12**.

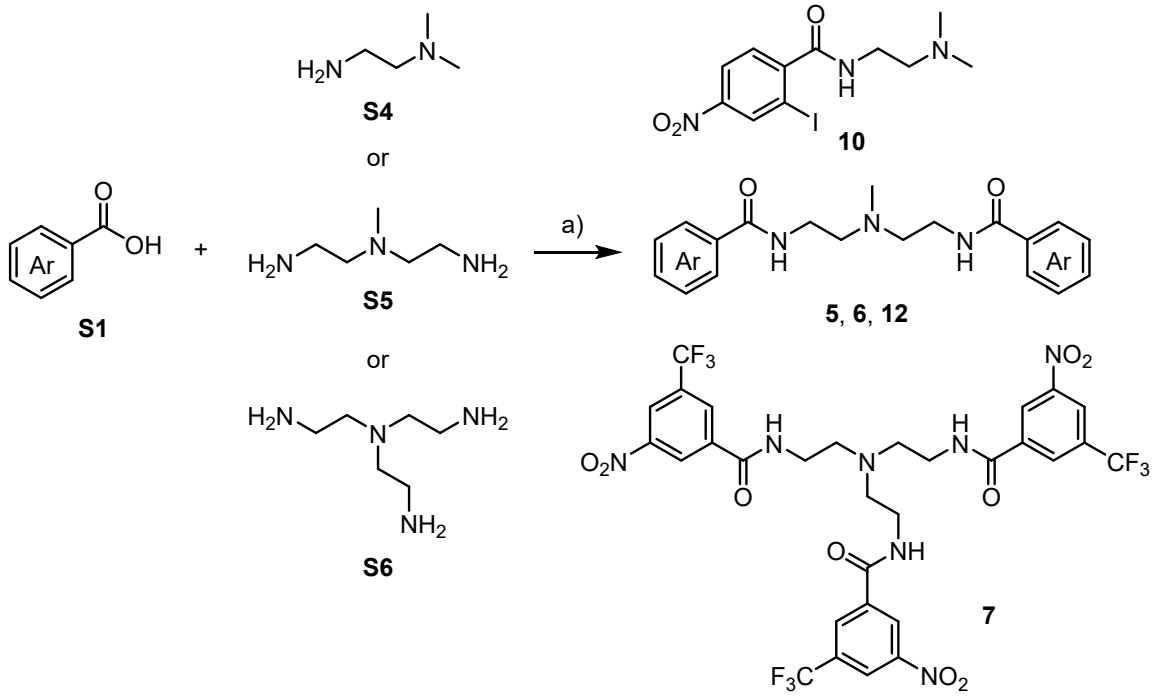

Scheme S2. (a) EDCI, DCM, rt, overnight

Compound 5 was obtained as a colorless solid, 1.2 g, 87%. Mp: 175 – 176 °C; IR (neat): 3299 (w), 3094 (w), 2914 (w), 2850 (w), 1647 (s), 1594 (w), 1540 (s), 1466 (m), 1436 (m),

1353 (w), 1326 (s), 1288 (s), 1175 (s), 1134 (s), 1110 (s), 912 (m), 788 (w), 739 (m), 721 (m), 687 (s); ^{1}H NMR (400 MHz, DMSO-d_6): 9.00 (t, J = 5.6 Hz, 2H), 8.85 (s, 2H), 8.60 (s, 2H), 8.55 (s, 2H), 3.43 (q, J = 6.3 Hz, 4H), 2.61 (t, J = 6.6 Hz, 4H), 2.32 (s, 3H); ^{13}C NMR (100 MHz, DMSO-d_6): 162.99, 148.68, 137.51, 130.89 (d, J = 33.6 Hz), 130.12, 126.25, 123.21 (d, J = 273.0 Hz), 123.13, 56.32, 42.67, 38.13; ^{19}F NMR (376 MHz, DMSO-d_6): -61.47; HRMS (ESI) calcd for $C_{21}H_{20}F_6N_5O_6^+$ ([M+H]$^+$): 552.1312, found: 552.1315.

Compound 6 was obtained as a caramel solid, 1.0 g, 79%. Mp: 171 – 174 ^{o}C; IR (neat): 3308 (w), 3097 (w), 2925 (w), 1647 (m), 1538 (s), 1458 (w), 1344 (s), 1310 (m), 1168 (w), 1077 (m), 919 (m), 729 (s), 720 (s); ^{1}H NMR (400 MHz, DMSO-d_6): 9.13 (t, J = 5.5 Hz, 2H), 8.99 (d, J = 2.1 Hz, 4H), 8.92 (t, J = 2.1 Hz, 2H), 3.44 (q, J = 6.3 Hz, 4H), 2.62 (t, J = 6.6 Hz, 4H), 2.32 (s, 3H). ^{13}C NMR (100 MHz, DMSO-d_6): 162.48, 148.55, 137.50, 127.84, 121.11, 56.30, 42.61, 38.19; HRMS (ESI) calcd for $C_{19}H_{20}N_7O_{10}^+$ ([M+H]$^+$): 506.1266, found: 506.1265.

Compound 7 was obtained as a colorless solid, 744 mg, 58%. Mp: 154 – 156 ^{o}C; IR (neat): 3294 (w), 2955 (w), 2923 (w), 1708 (w), 1647 (m), 1540 (s), 1465 (w), 1435 (w), 1354 (w), 1327 (s), 1275 (s), 1261 (s), 1175 (m), 1135 (s), 1111 (m), 912 (w), 764 (s), 750 (s), 723 (w), 687 (m); ^{1}H NMR (400 MHz, DMSO-d_6): 9.00 (t, J = 5.4 Hz, 3H), 8.78 (d, J = 1.9 Hz, 3H), 8.55 (t, J = 2.0 Hz, 3H), 8.47 (d, J = 1.7 Hz, 3H), 3.46 (q, J = 6.1 Hz, 6H), 2.78 (t, J = 6.3 Hz, 6H); ^{13}C NMR (100 MHz, DMSO-d_6): 163.17, 148.54, 137.45, 130.81 (q, J = 33.6 Hz), 130.09, 126.19, 123.14 (d, J = 272 Hz), 123.03, 53.65, 38.58; ^{19}F NMR (376 MHz, DMSO-d_6): -61.65; HRMS (ESI) calcd for $C_{30}H_{25}F_9N_7O_9^+$ ([M+H]$^+$): 798.1565, found: 798.1566.

Compound 10 was obtained as a yellow solid, 1.5 g, 83%. Mp: 138 – 140 °C; IR (neat): 3265 (w), 3090 (w), 2945 (w), 2859 (w), 2823 (w), 2779 (w), 1646 (s), 1584 (w), 1521 (s), 1460 (m), 1346 (s), 1308 (w), 1250 (w), 1191 (w), 1112 (w), 1039 (w), 844 (m), 726 (m); ^{1}H NMR (400 MHz, $CDCl_3$): 8.69 (d, J = 2.2 Hz, 1H), 8.23 (dd, J = 8.4, 2.2 Hz, 1H), 7.54 (d, J = 8.4 Hz, 1H), 6.53 (s, 1H), 3.59 – 3.49 (m, 2H), 2.57 – 2.49 (m, 2H), 2.26 (s, 6H); ^{13}C NMR (100 MHz, $CDCl_3$): 167.72, 148.10, 134.58, 128.72, 123.20, 92.23, 57.18, 45.00, 37.20 (one carbon signal missing because of peak overlap); HRMS (ESI) calcd for $C_{11}H_{15}IN_3O_3^+$ ($[M+H]^+$): 364.0153, found: 364.0156.

Compound 12 was obtained as a yellow solid, 350 mg, 61%. Mp: 180 – 182 °C; IR (neat): 3265 (w), 3090 (w), 2927 (w), 2849 (w), 1640 (s), 1584 (w), 1520 (s), 1460 (w), 1345 (s), 1313 (w), 1283 (w), 1250 (w), 1208 (w), 1172 (w), 1111 (w), 1040 (w), 895 (w), 843 (m), 728 (m), 653 (w); ^{1}H NMR (400 MHz, $CDCl_3$): 7.92 (d, J = 1.7 Hz, 2H), 7.51 (dd, J = 8.0, 1.7 Hz, 2H), 7.37 (d, J = 7.9 Hz, 2H), 6.55 (d, J = 5.3 Hz, 2H), 3.53 (q, J = 5.6 Hz, 4H), 2.67 (t, J = 5.8 Hz, 4H), 2.32 (s, 3H); ^{13}C NMR (100 MHz, $CDCl_3$): 168.56, 145.35, 136.40, 132.78 (d, J = 33.4 Hz), 128.60, 125.09, 122.37 (d, J = 273.1 Hz), 92.29, 56.03, 41.79, 37.38; ^{19}F NMR (376 MHz, $CDCl_3$): -63.09; HRMS (ESI) calcd for $C_{21}H_{20}F_6I_2N_3O_2^+$ ($[M+H]^+$): 713.9544, found: 713.9543.

Compound 13 and **14** were synthesized following the general procedure below (Scheme S3). To a solution of aryl acid **S7** (10.0 mmol) in DCM (40 mL) was added EDCI (2.0 g, 10.6 mmol) at rt, followed by the addition of *N*-boc-ethylenediamine (1.6 g, 10.0 mmol). The reaction mixture was stirred at this temperature for 4 h. The resulting mixture was extracted with DCM (100 mL × 3). The combined organic layers were washed with saturated $NaHCO_3$

(50 mL) and brine (50 mL), dried over Na_2SO_4 and concentrated *in vacuo* to give intermediate **S8**. Then 100 mL of 1.0 M NaOH was added and the mixture was stirred at rt overnight. The resulting mixture was acidified by 3.0 M HCl to pH 3.0-5.0 and extracted with EtOAc (100 mL × 3). The combined organic layers were washed with saturated $NaHCO_3$ (50 mL) and brine (50 mL), dried over Na_2SO_4 and concentrated *in vacuo*. To a solution of the residue in DCM (40 mL) was added EDCI (2.0 g, 10.6 mmol) at rt, followed by the addition of **S5** (1.17 g, 10 mmol). The reaction mixture was stirred at this temperature for 4 h. The resulting mixture was extracted with DCM (100 mL × 3). The combined organic layers were washed with saturated $NaHCO_3$ (50 mL) and brine (50 mL), dried over Na_2SO_4 and concentrated *in vacuo* to give intermediate **S9**. Then the solution of **S9** in DCM was added TFA (TFA:DCM=1:4) at 0 ºC and stirred at 0 ºC-rt for 1 h. The resulting mixture was concentrated in vacco. The residue was added to the mixture of **S1** (10 mmol), EDCI (2.0 g, 10.6 mmol), HOBt (1.4 g, 10.6 mmol) and Et_3N (1.4 mL, 10 mmol) in DCM (mL) at rt. The mixture was stirred at this temperature overnight and then extracted with DCM (100 mL × 3). The combined organic layers were washed with saturated $NaHCO_3$ (50 mL) and brine (50 mL), dried over Na_2SO_4 and concentrated *in vacuo*. The residue was purified by column chromatography on silica gel using DCM/MeOH (90:10) as eluent to give pure compounds **13** and **14**.

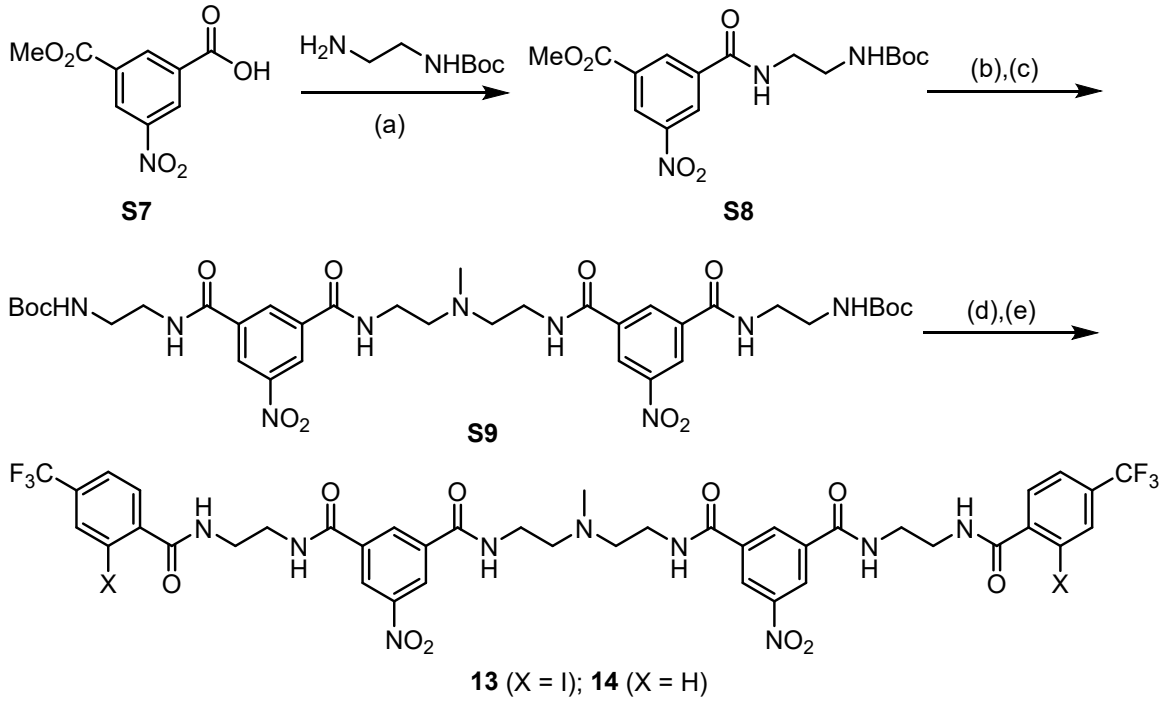

Scheme S3. (a) EDCI, DCM, rt, 4 h; (b) NaOH (1.0 M), rt, overnight; (c) EDCI, DCM, **S5**, overnight; (d) TFA, DCM, 0 ^{o}C-rt, 1 h; (e) **S1**, EDCI, HOBt, Et_3N, DCM, then **S9**.

Compound 13 was obtained as a light yellow solid, 1.4 g, 24% (over 5 steps). Mp: >250 ^{o}C; IR (neat): 3257 (w), 3084 (w), 1649 (s), 1554 (m), 1531 (m), 1451 (w), 1349 (w), 1322 (s), 1298 (w), 1268 (w), 1185 (w), 1125 (m), 1076 (w), 915 (w), 882 (w), 841 (w), 817 (w), 750 (w), 728 (w), 699 (w), 640 (w); ^{1}H NMR (400 MHz, DMSO-d_6): 9.07 (t, J = 5.3 Hz, 2H), 8.92 (d, J = 5.7 Hz, 2H), 8.82 – 8.65 (m, 8H), 8.19 (s, 2H), 7.84 (d, J = 8.6 Hz, 2H), 7.58 (d, J = 8.0 Hz, 2H), 3.54 – 3.36 (m, 12H), 2.62 (s, 4H), 2.33 (s, 3H); ^{13}C NMR (100 MHz, DMSO-d_6): 168.71, 164.41, 164.08, 148.19, 147.49, 136.57, 136.52, 135.80, 132.80, 131.03 (d, J = 32.3 Hz), 129.03, 125.46, 124.59, 123.2 (q, J = 263 Hz), 116.98, 94.67, 56.36, 42.58, 39.02, 37.96 (one carbon signal missing because of peak overlap); ^{19}F NMR (376 MHz, DMSO-d_6): -61.31. HRMS (ESI) calcd for $C_{41}H_{38}F_6I_2N_9O_{10}^+$ ([M+H]$^+$): 1184.0730, found: 1184.0732.

Compound 14 was obtained as a light yellow solid, 1.2 g, 26% (over 5 steps). Mp: 200 –

203 °C; IR (neat): 3293 (w), 3084 (w), 2944 (w), 1641 (s), 1530 (s), 1436 (w), 1408 (w), 1323 (s), 1165 (s), 1124 (s), 1067 (s), 1016 (s), 918 (w), 859 (m), 772 (w), 721 (m), 684 (m), 598 (m); ^{1}H NMR (400 MHz, DMSO-d_6): 9.14 (brs, 2H), 8.93 – 8.90 (m, 4H), 8.76 (s, 2H), 8.73 (s, 2H), 8.71 (s, 2H), 8.04 (d, J = 8.1 Hz, 4H), 7.84 (d, J = 7.9 Hz, 4H), 3.58 – 3.45 (m, 12H), 2.60 (t, J = 6.8 Hz, 4H), 2.31 (s, 3H); ^{13}C NMR (100 MHz, DMSO-d_6): 165.87, 164.43, 164.08, 148.16, 138.71, 136.56, 136.52, 132.72, 131.53 (q, J = 31.7 Hz), 128.60, 127.16 (q, J = 288.0 Hz), 125.76, 124.56, 124.51, 56.35, 42.59, 37.98 (two carbon signals missing because of peak overlap); ^{19}F NMR (376 MHz, DMSO-d_6): -61.33. HRMS (ESI) calcd for $C_{41}H_{40}F_6N_9O_{10}^+$ ([M+H]$^+$): 932.2797, found: 932.2799.

3. Catalysis

3.1 Decarboxylative Michael Addition

3.1.1 ^{1}H NMR Kinetics

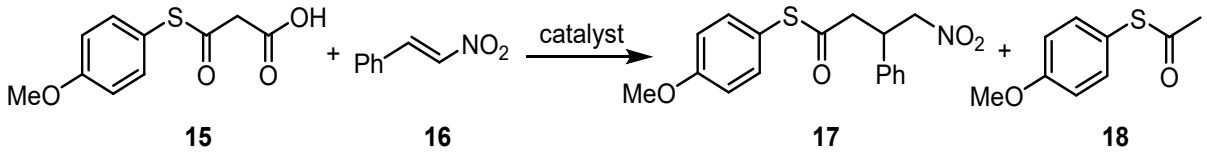

15 **16** **17** **18**

Scheme S4. Catalytic reaction of malonic acid half thioester (MAHT) **15** with nitroolefin **16**.

The kinetics were studied following a previously published protocol.[S4,S5] Solutions comprising substrates **15** (200 mM) and **16** (2.0 M) and catalyst (20 mM as a representative example) were prepared in $CDCl_3$/THF-d_8 (1:1) and stirred at 20 °C. ^{1}H NMR spectra of the mixture (10 μL) diluted in $CDCl_3$ (0.6 mL) were recorded over time (Figures S1). Integrals associated with the protons alpha to the carbonyl group of the addition product **17** (δ 3.07 ppm; d, 2H) and decarboxylation (δ 2.38 ppm; s, 3H) were observed. Integrals were normalized against the combined integration of all –OCH_3 protons present in the substrates and products (i.e., from δ 3.84–3.79 ppm). Concentrations of products **17** and **18** were plotted against time (Table S1), and the initial velocities were determined from the linear fitting (Figure S2).

3.1.2 Catalyst Evaluation

The catalysts were evaluated and summarized in Figures S3, S4 and Table S1. Solutions comprising substrates **15** (200 mM) and **16** (2.0 M) and catalyst **13** (2, 10, 20, 40 mM) were prepared in $CDCl_3$/THF-d_8 (1:1) and stirred at 20 °C for 24 h. ^{1}H NMR spectra of the mixture (10 μL) diluted in $CDCl_3$ (0.6 mL) were recorded (Figures S3 and S5). The concentration of

the products **17** and **18** was determined from the integration of pertinent resonances as mentioned above. Yields (η) and addition/decarboxylation ratio (A/D) for MAHT addition were determined from the ratio of addition to decarboxylation products measured at the end of the reaction (Equations S1 and S2, Figure S4 and S6, Table S1).

$$\eta = \frac{\int addition + \int Decarboxytation}{\int (-OCH_3)} \times \frac{H_D}{H_A} \times 100\% \quad \text{(S1)}$$

$$A/D = \frac{\int addition}{\int Decarboxylation} \times \frac{H_D}{H_A} \quad \text{(S2)}$$

here H_A = 2.0 and H_D = 3.0 for integrals measured at δ 3.07 and 2.38 ppm, respectively.

3.1.3 Solvent Screening

The MAHT reaction were conducted in different solvents ($CDCl_3$, THF-d_8, $CDCl_3$/THF-d_8) for 24 h. ^{1}H NMR spectra of the mixture (10 μL) diluted in $CDCl_3$ (0.6 mL) were recorded (Figure S7) and the yield (η) and A/D ratio were estimated (Figure S8) as mentioned above and then summarized in Table S1.

3.1.4 Nitrate Inhibition

Solutions comprising substrates **15** (200 mM) and **16** (2.0 M), catalyst **13** (20 mM) and $TBANO_3$ (200, 400, 800 mM) were prepared in $CDCl_3$/THF-d_8 (1:1) and stirred at 20 ^{o}C for 24 h. ^{1}H NMR spectra of the mixture (10 μL) diluted in $CDCl_3$ (0.6 mL) were recorded (Figure S9) and the yield (η) and A/D ratio were estimated (Figure S10) as mentioned above and then summarized in Table S1.

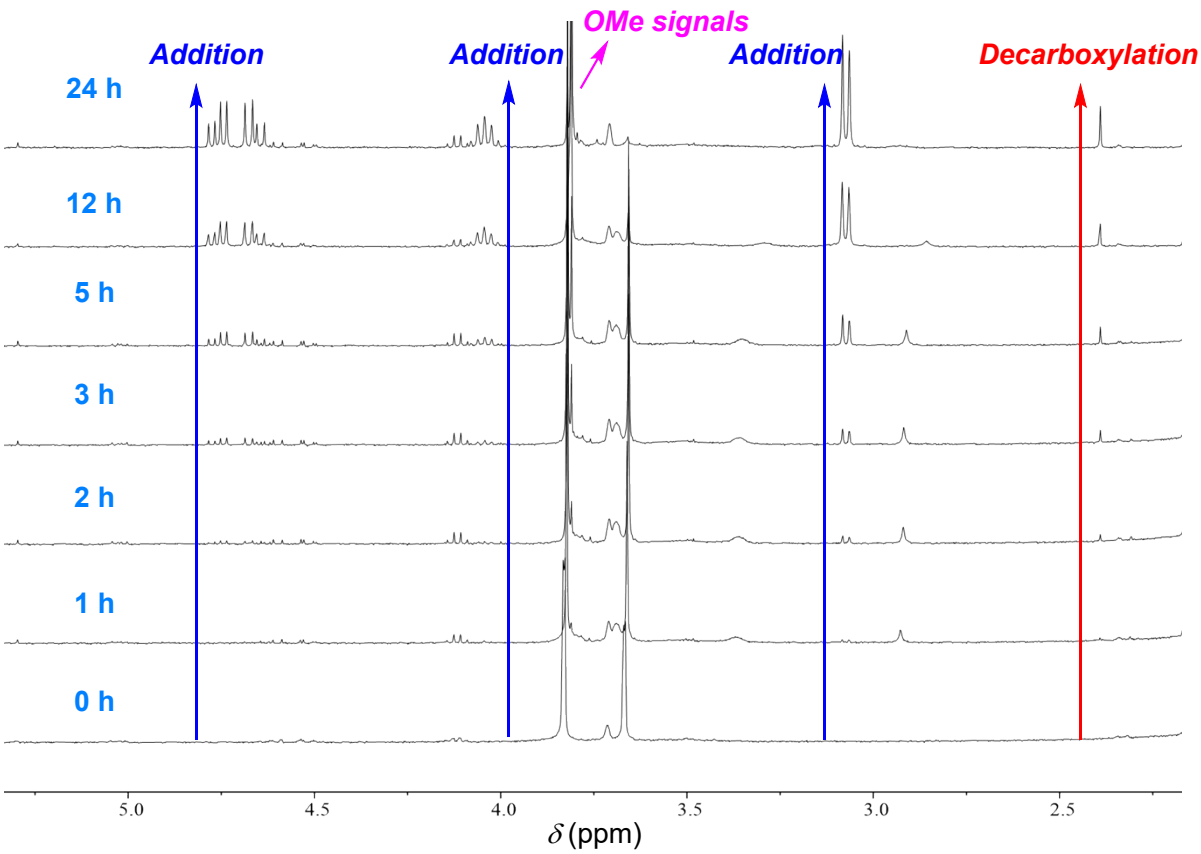

Figure S1. ^{1}H NMR spectra of a mixture of substrates **15** (200 mM) and **16** (2.0 M) and **13** (20 mM) in $CDCl_3$/THF-d_8 (1:1) at 20 °C diluted in $CDCl_3$. The blue arrows show the formation of **16** (addition), the red one shows the generation of product **18** (decarboxylation) and the pink arrow show the OMe signals in substrate **15** and products **17** and **18**.

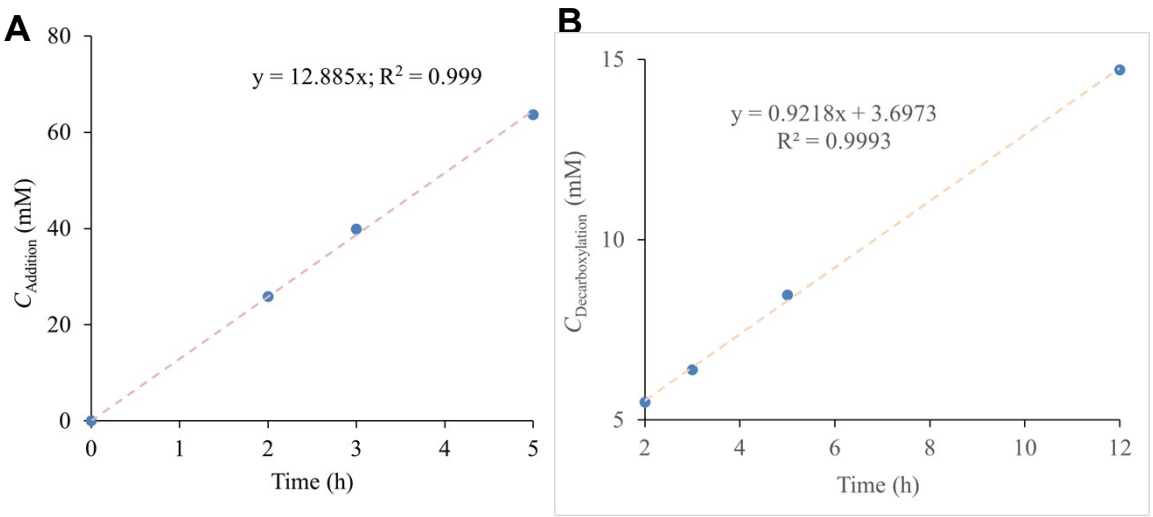

Figure S2. Plots of concentration of products **17** (A) and **18** (B) against time using **13** as catalyst (10 mol%) in $CDCl_3$/THF-d_8 (1:1) at 20 °C.

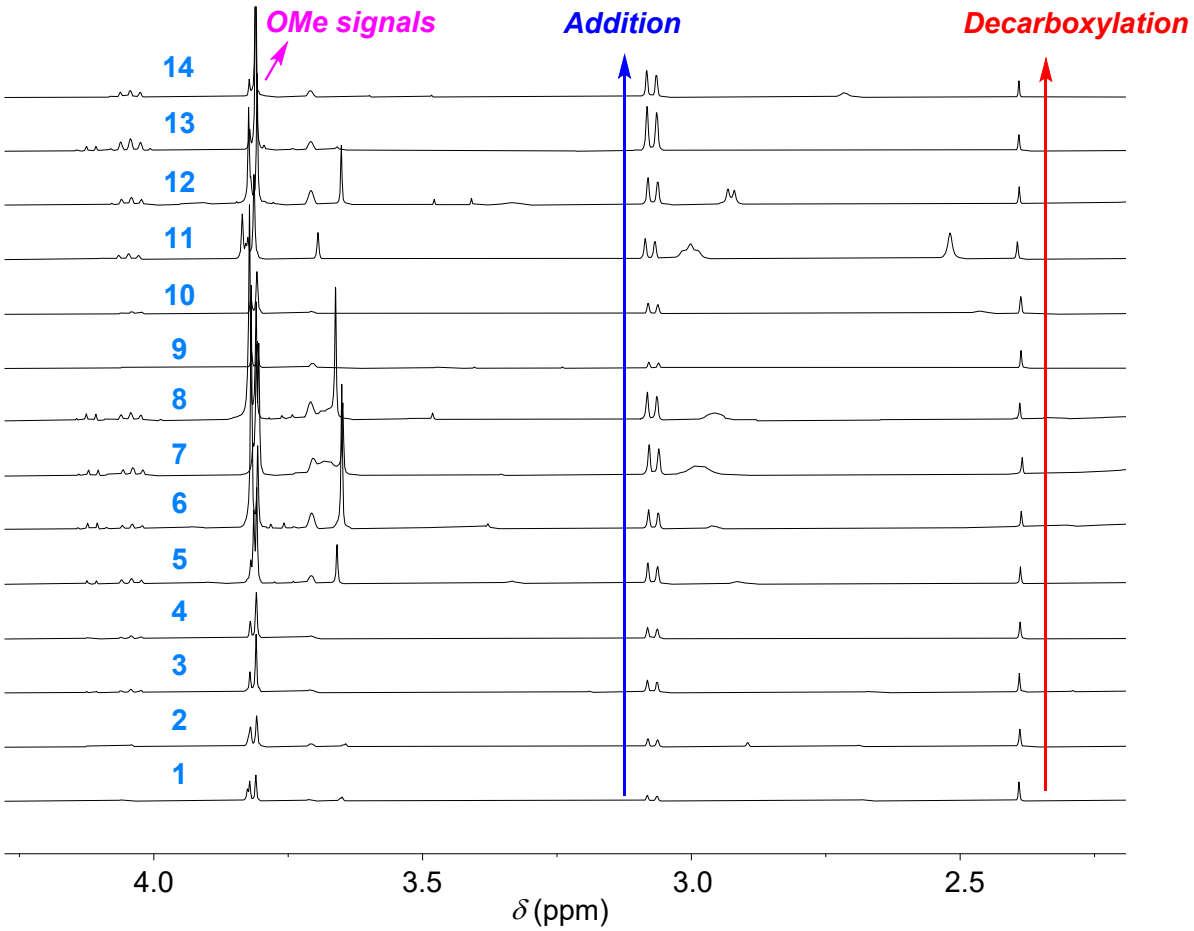

Figure S3. ^{1}H NMR spectra of a mixture of substrates **15** (200 mM) and **16** (2.0 M) and catalysts **1-14** (20 mM) in $CDCl_3$/THF-d_8 (1:1) at 20 °C for 24 h diluted in $CDCl_3$. The blue arrows show the formation of **17**, the red one shows the generation of **18** and the pink arrow show the OMe signals in **15**, **17** and **18**.

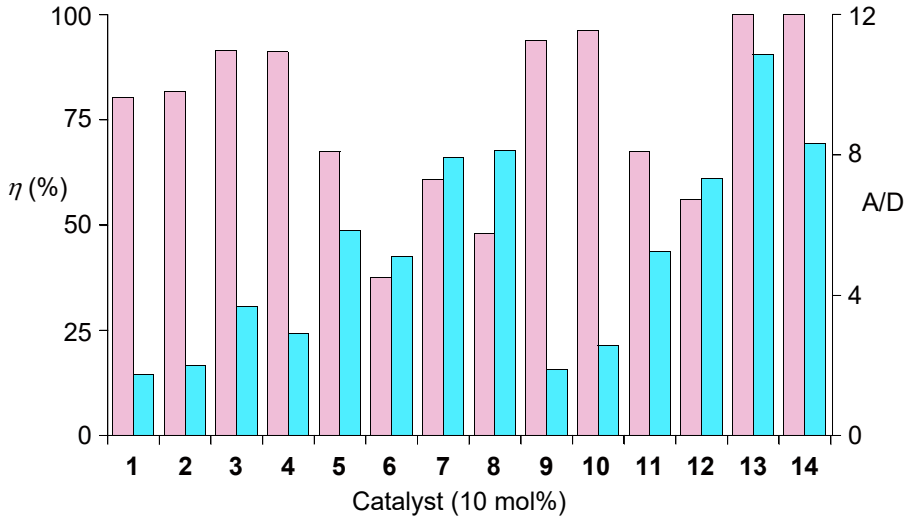

Figure S4. Reaction yields and A/D selectivity of the MAHT reactions catalyzed by **1-14** (10 mol%) in $CDCl_3$/THF-d_8 (1:1) at 20 °C for 24 h.

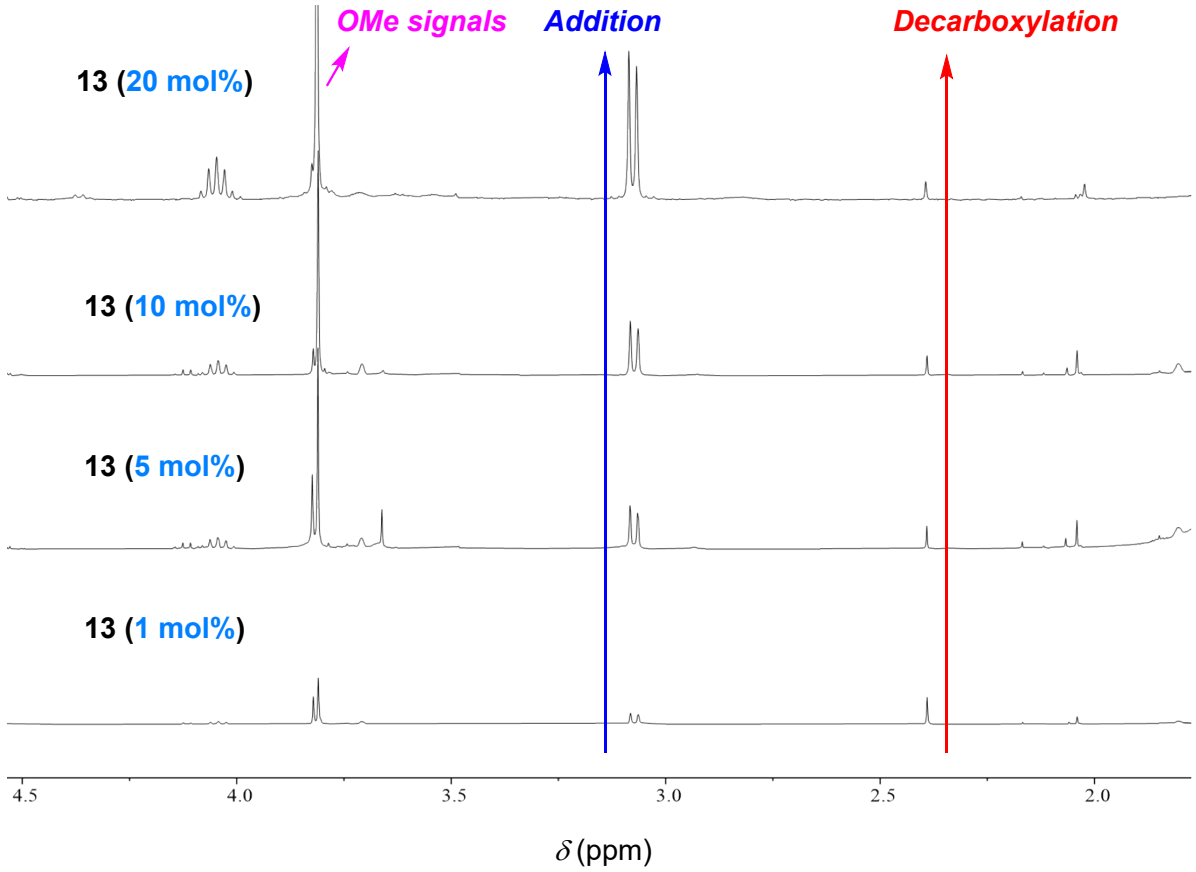

Figure S5. ^{1}H NMR spectra of a mixture of substrates **15** (200 mM) and **16** (2.0 M) and catalyst **13** (2, 10, 20, 40 mM) in $CDCl_3$/THF-d_8 (1:1) at 20 °C for 24 h diluted in $CDCl_3$. The blue arrows show the formation of **17**, the red one shows the generation of **18** and the pink arrow show the OMe signals in **15**, **17** and **18**.

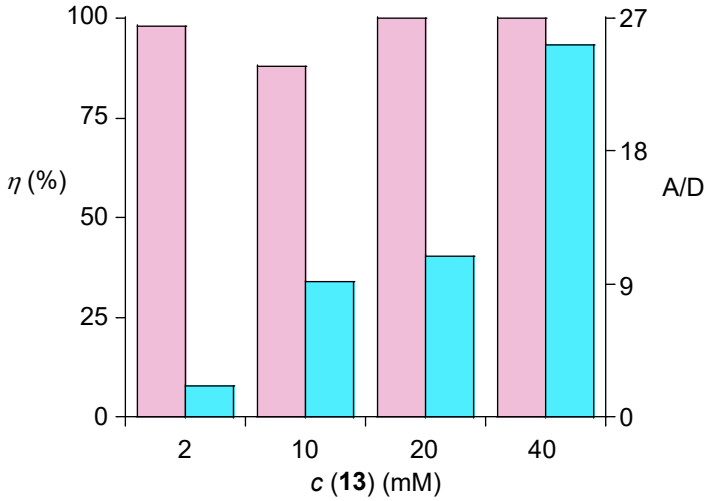

Figure S6. Reaction yields and A/D selectivity of the MAHT reactions catalyzed by **13** (1, 5, 10, 20 mol%) in $CDCl_3$/THF-d_8 (1:1) at 20 °C for 24 h.

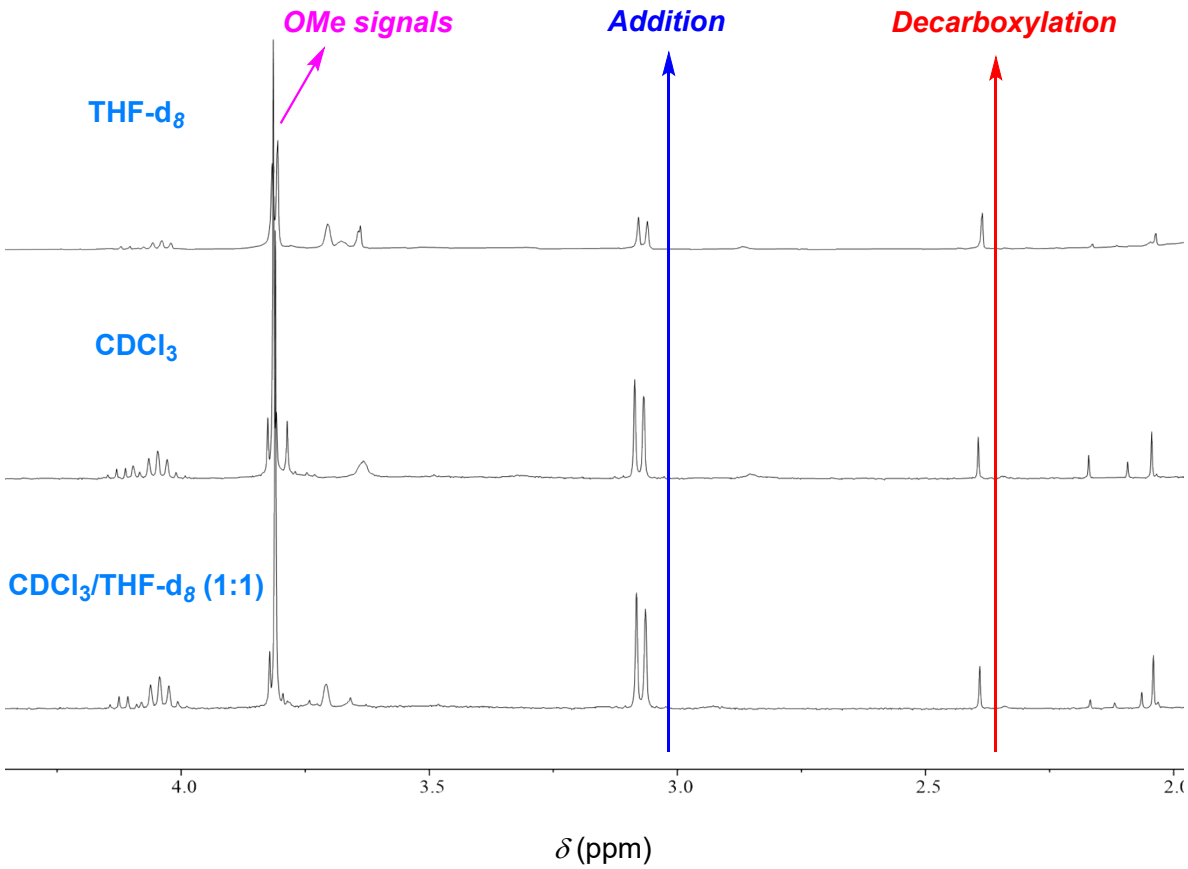

Figure S7. ^{1}H NMR spectra of a mixture of substrates **15** (200 mM) and **16** (2.0 M) and catalyst **13** (20 mM) in different solvents at 20 °C for 24 h diluted in $CDCl_3$. The blue arrows show the formation of **17**, the red one shows the generation of **18** and the pink arrow show the OMe signals in **15**, **17** and **18**.

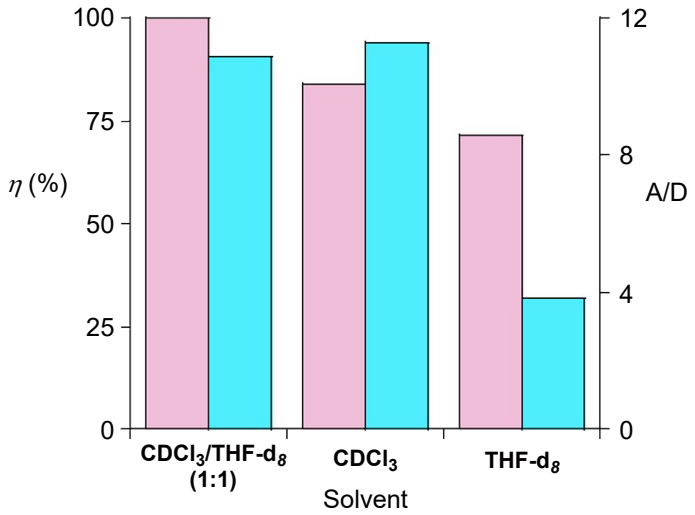

Figure S8. Reaction yields and A/D selectivity of the MAHT reactions catalyzed by **13** (10 mol%) in different solvents at 20 °C for 24 h.

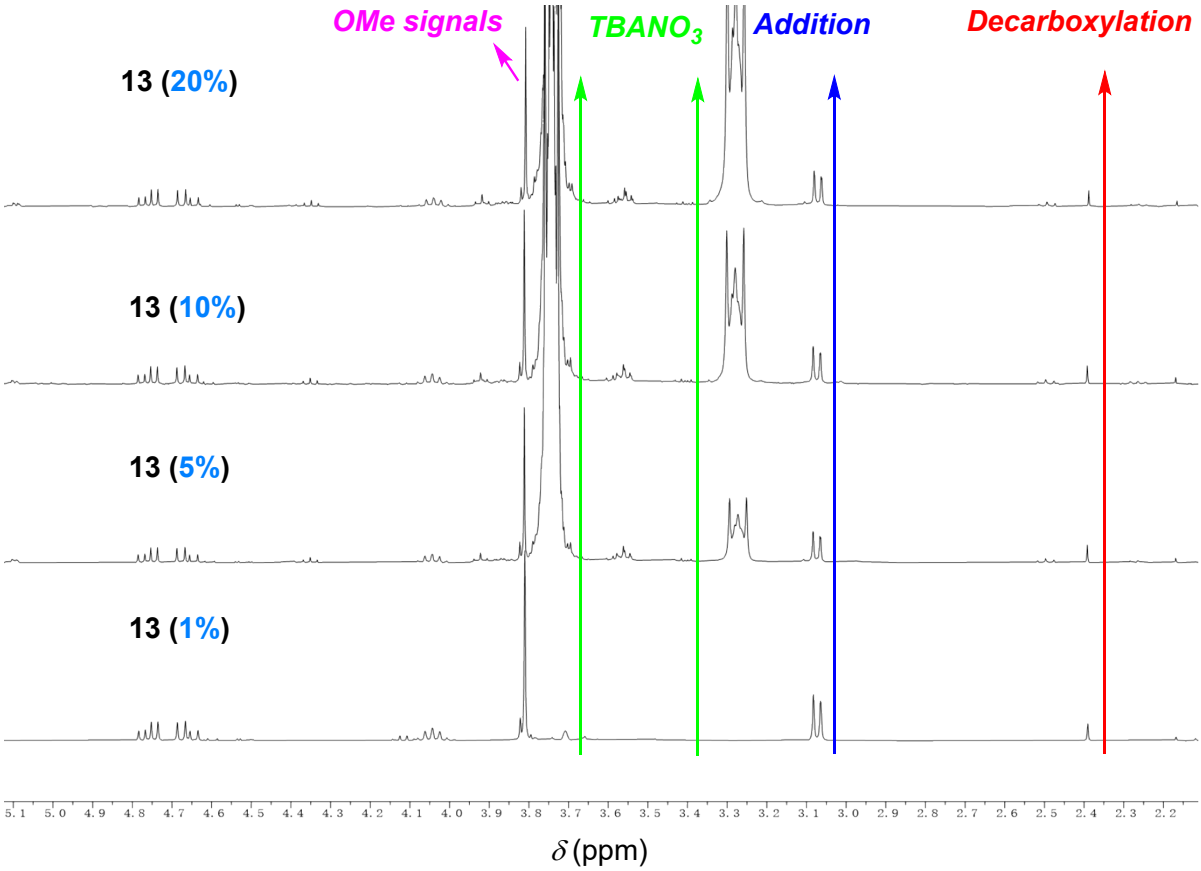

Figure S9. ^{1}H NMR spectra of a mixture of substrates **15** (200 mM) and **16** (2.0 M) and catalyst **13** (20 mM) in $CDCl_3$/THF-d_8 (1:1) at 20 °C for 24 h diluted in $CDCl_3$. The blue arrows show the formation of **17**, the green arrows represent the peaks of $TBANO_3$, the red one shows the generation of **18** and the pink arrow show the OMe signals in **15**, **17** and **18**.

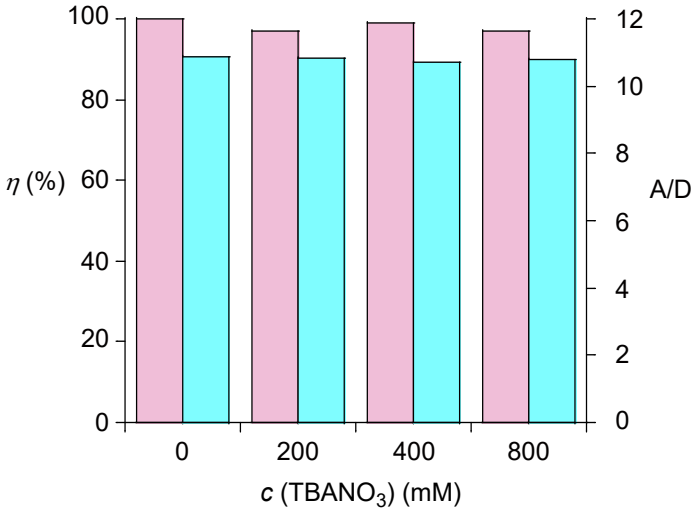

Figure S10. Reaction yields and A/D selectivity of the MAHT reactions catalyzed by **13** (10 mol%) with $TBANO_3$ (1.0, 2.0, 4.0 eq) in $CDCl_3$/THF-d_8 (1:1) at 20 °C for 24 h.

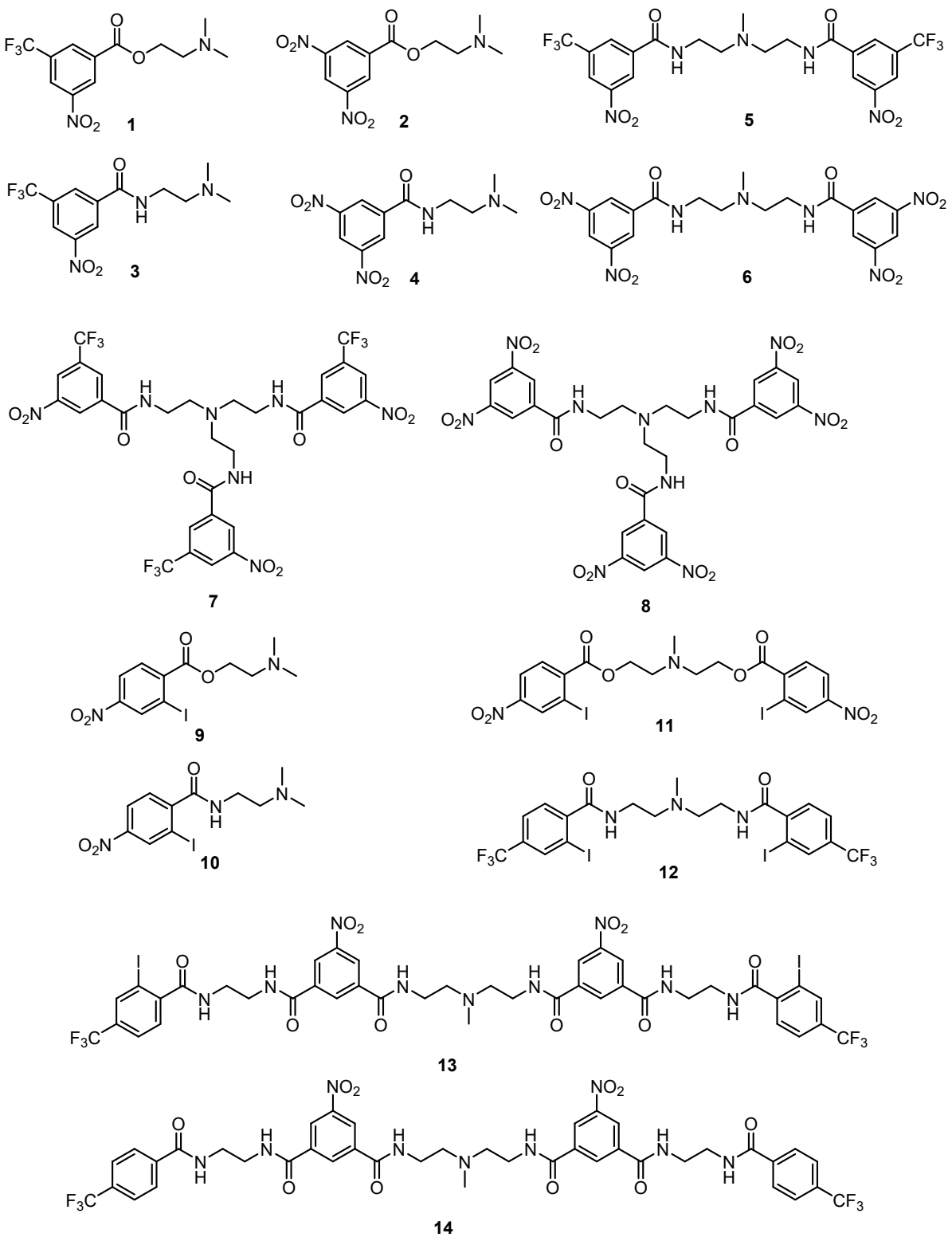

Figure S11. Chemical structures of catalysts **1-14**.

Table S1. Anion-π catalysis with halogen binding on MAHT reactions.[a]

	Cat[b]	*c* (Cat)[c]	S[d]	*c* (**16**)[e]	*c* (**17**)[f]	*η* (%)[g]	A/D[h]
1	**1**	20	$CDCl_3$/THF-d_8 (1:1)	102.1	58.7	80%	1.7
2	**2**	20	$CDCl_3$/THF-d_8 (1:1)	108.8	54.9	82%	2.0
3	**3**	20	$CDCl_3$/THF-d_8 (1:1)	143.8	39.1	91%	3.7
4	**4**	20	$CDCl_3$/THF-d_8 (1:1)	135.7	46.6	91%	2.9
5	**5**	20	$CDCl_3$/THF-d_8 (1:1)	115.3	19.8	68%	5.8
6	**6**	20	$CDCl_3$/THF-d_8 (1:1)	62.8	12.3	38%	5.1
7	**7**	20	$CDCl_3$/THF-d_8 (1:1)	108.0	13.6	61%	7.9
8	**8**	20	$CDCl_3$/THF-d_8 (1:1)	85.6	10.5	48%	8.1
9	**9**	20	$CDCl_3$/THF-d_8 (1:1)	122.5	65.4	94%	1.9
10	**10**	20	$CDCl_3$/THF-d_8 (1:1)	138.6	54.1	96%	2.6
11	**11**	20	$CDCl_3$/THF-d_8 (1:1)	113.4	21.7	68%	5.2
12	**12**	20	$CDCl_3$/THF-d_8 (1:1)	98.7	13.4	56%	7.3
13	**13**	20	$CDCl_3$/THF-d_8 (1:1)	185.2	17.1	100%	10.9
14	**14**	20	$CDCl_3$/THF-d_8 (1:1)	178.6	21.4	100%	8.3
15	**13**	2	$CDCl_3$/THF-d_8 (1:1)	132.3	63.9	98%	2.1
16	**13**	10	$CDCl_3$/THF-d_8 (1:1)	158.8	17.3	88%	9.2
17	**13**	40	$CDCl_3$/THF-d_8 (1:1)	192.7	7.7	100%	25.2
18	**13**	20	$CDCl_3$	154.4	13.7	84%	11.3
19	**13**	20	THF-d_8	113.5	29.7	72%	3.8
20[i]	**13**	20	$CDCl_3$/THF-d_8 (1:1)	176.7	16.3	97%	10.8
21[i]	**13**	20	$CDCl_3$/THF-d_8 (1:1)	180.5	16.8	99%	10.7
22[i]	**13**	20	$CDCl_3$/THF-d_8 (1:1)	178.1	16.5	97%	10.8
23[j]	**TEA**	40	$CDCl_3$/THF-d_8 (1:1)	-	-	-	1.8

[a]Measured with substrates **15** (200 mM) and **16** (2.0 M) and catalyst (see columns **Cat** and *c* (Cat)) in a solvent at 20 °C. [b]Catalysts, see Figure S11. [c]Catalyst concentrations (mM). [d]Solvents. [e]Concentration of product **17** (mM). [f]Concentration of product **18** (mM). [g]NMR yields (%). [h]Ratio of addition (A) and decarboxylation (D) products. [i]$TBANO_3$ (1.0, 2.0 and 4.0 eq for entries 19-21, respectively) was added. [j]Data originated from reference S6.

3.2 Michael Addition Reaction (Focus on Nonadjacent Stereocenters)[S7]

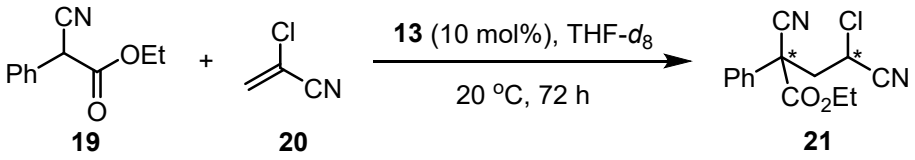

Scheme S5. Michael addition reaction between **19** and **20**

The solution of substrate **19** (0.5 M), substrate **20** (2.0 M), internal standard dibromomethane (0.5 M) and catalyst **13** (50 mM) was prepared in THF-d_8 and stirred at 20 °C. ^{1}H NMR spectra of the mixture diluted in $CDCl_3$ were recorded after 72 h (Figure S12). The conversion of the substrate **19** was determined by comparing the integration of pertinent resonances (e.g. 4.65 ppm, 4.58 ppm) with those of internal standards in the crude NMR spectrum. Diastereoselectivity of **21** was determined from the integrals of pertinent peaks in crude NMR spectra of the reaction mixtures (Figure S13).

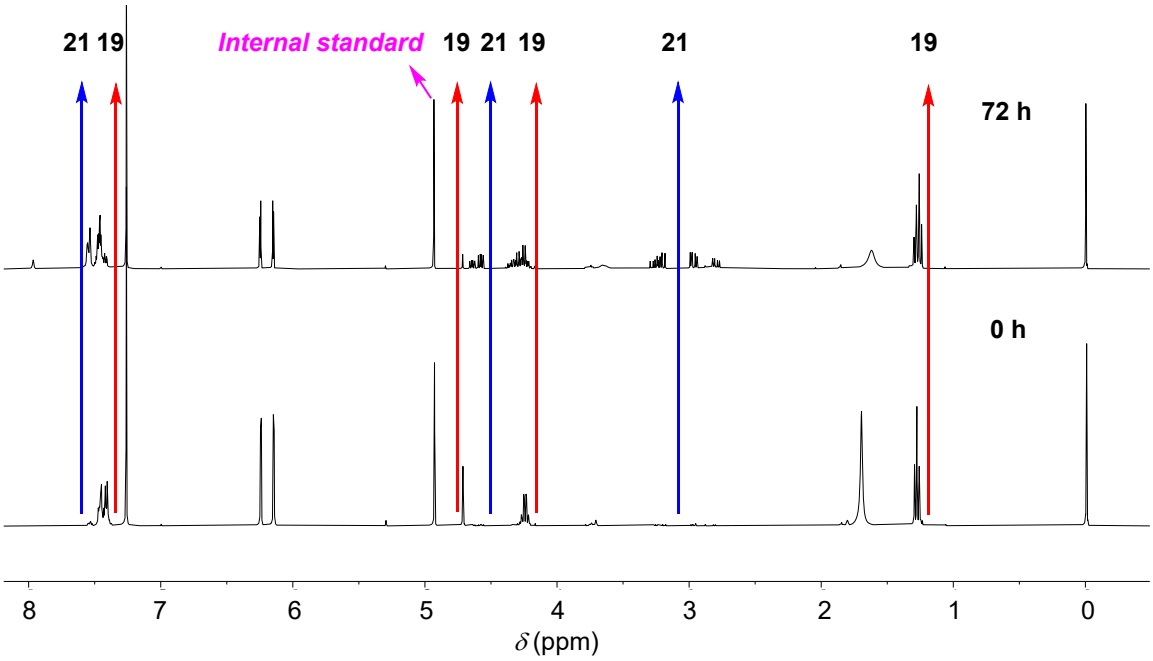

Figure S12. ^{1}H NMR spectra of a mixture of substrates **19** (0.5 M) and **20** (2.0 M), internal standard dibromomethane (0.5 M) and catalyst **13** (20 mM) in $CDCl_3$/THF-d_8 (1:1) at 20 °C for 72 h diluted in $CDCl_3$. The blue arrows show the formation of **21**, the red one shows the consumption of **19** and the pink arrow show the signal of internal standard.

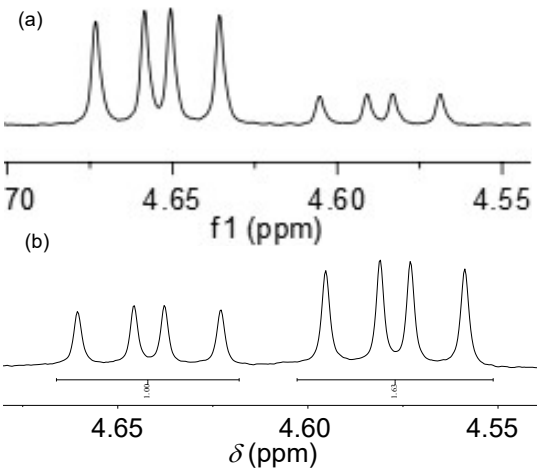

Figure S13. Diagnostic regions of crude ^{1}H NMR spectrum of the reaction mixture of **19** and **20** used to determine diastereoselectivity of **21** in the presence of (a) cinchona-alkaloid[S7] and (b) catalyst **13**.

3.3 Diels-Alder Reaction[S8]

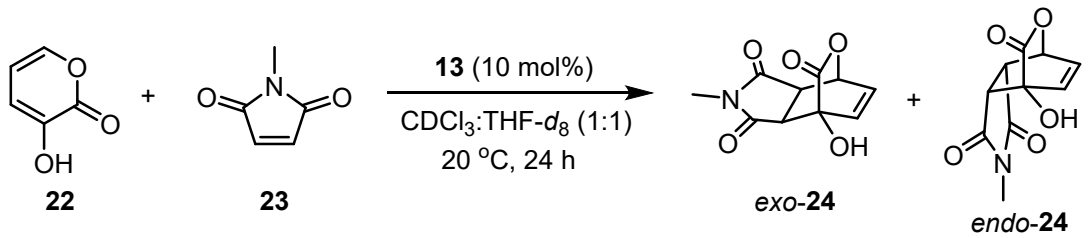

Scheme S6. Diels-Alder reaction between **22** and **23**

The solution of substrates **22** (0.5 M) and maleimide **23** (1.0 M), internal standard dibromomethane (0.5 M) and catalyst **13** (50 mM) was prepared in $CDCl_3$/THF-d_8 (1:1) and stirred at 20 °C. ^{1}H NMR spectra of the mixture diluted in $CDCl_3$ were recorded after 24 h (Figure S14). The concentration of products *exo*-**24** and *endo*-**24** was determined by comparing the integration of pertinent resonances with those of internal standards in the crude NMR. Diastereoselectivity between the *exo* and *endo* isomers was determined from the integrals of pertinent peaks in crude NMR spectra of the reaction mixtures (Figure S15).

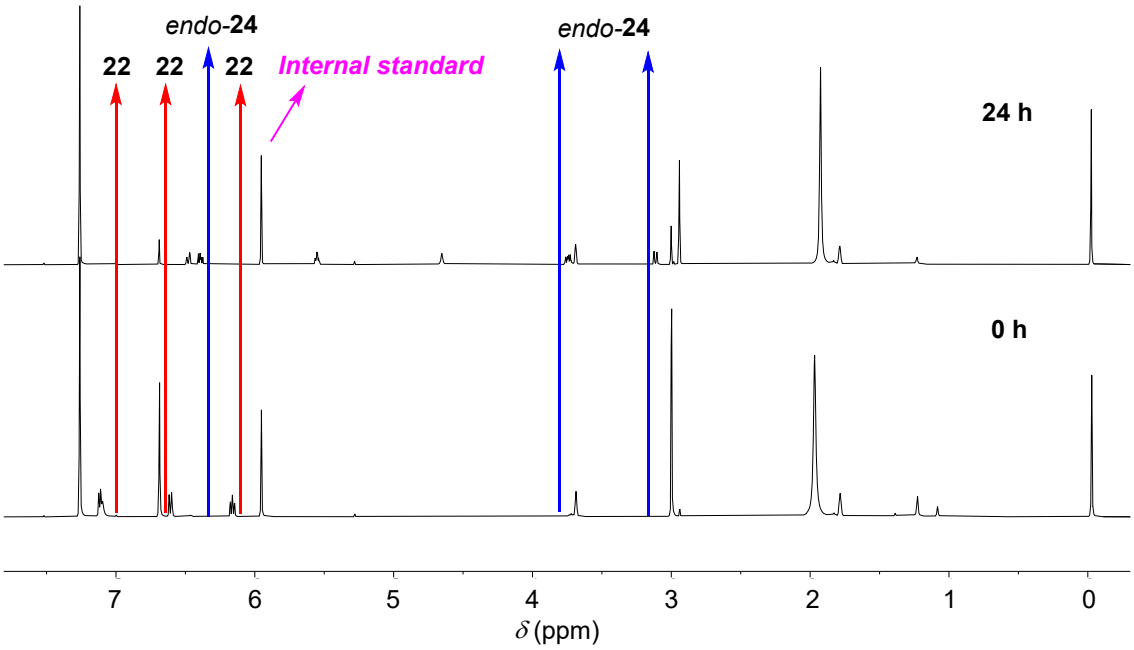

Figure S14. ^{1}H NMR spectra of a mixture of substrates **22** (0.5 mM) and **23** (1.0 M) and catalyst **13** (50 mM) in $CDCl_3$/THF-d_8 (1:1) at 20 °C for 24 h diluted in $CDCl_3$. The blue arrows show the formation of *endo*-**24**, the red one shows the consumption of **22** and the pink arrow show the signal of internal standard.

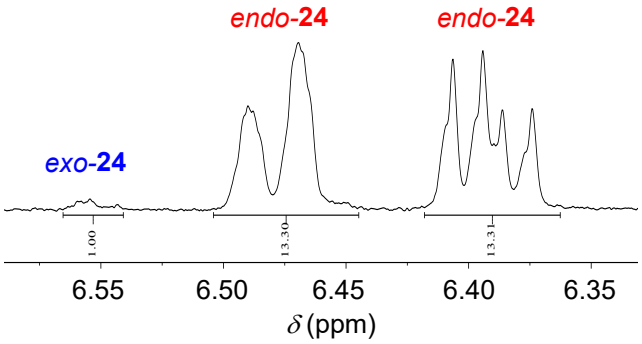

Figure S15. Diagnostic regions of crude ^{1}H NMR spectrum of the reaction mixture of **22** and **23** used to determine the diastereoselectivity of **24** catalyzed by **13**.

3.4 [3+2] Cycloaddition Reaction[S9]

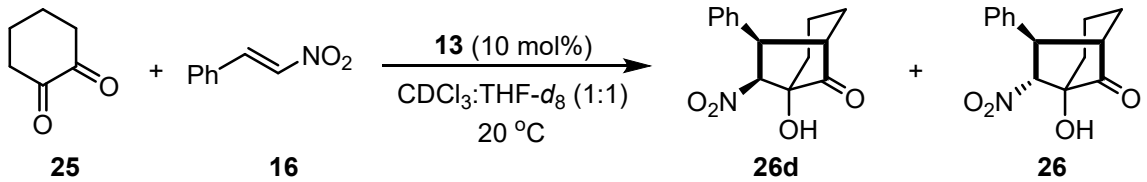

25 **16** **26d** **26**

Scheme S7. [3+2] Cycloaddition Reaction between **25** and **16**

The solutions of substrates **25** (0.4 M) and **16** (0.8 M), internal standard dibromomethane (0.4 M) and catalyst **13** (40 mM) was prepared in $CDCl_3$/THF-d_8 (1:1) and stirred at 20 °C. ^{1}H NMR spectra of the mixture diluted in $CDCl_3$ were recorded after 24 h (Figure S16). The concentration of the products **26** and **26d** was determined by comparing the integration of pertinent resonances with those of internal standards in the crude NMR. Diastereoselectivity between the major isomers **26** and **26d** was determined from the integrals of pertinent peaks in crude NMR spectra of the reaction mixtures (Figure S17).

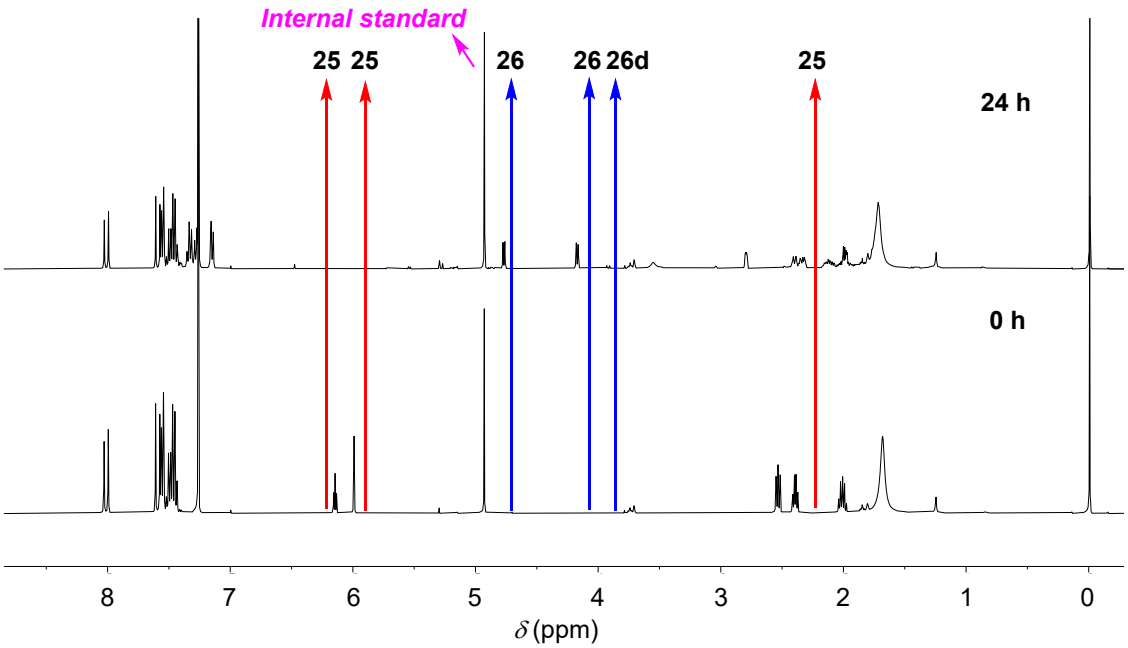

Figure S16. ^{1}H NMR spectra of a mixture of substrates **25** (0.4 M) and **16** (0.8 M) and catalyst **13** (40 mM) in $CDCl_3$/THF-d_8 (1:1) at 20 °C for 24 h diluted in $CDCl_3$. The blue arrows show the formation of **26** and **26d**, the red one shows the consumption of **25** and the pink arrow show the signal of internal standard.

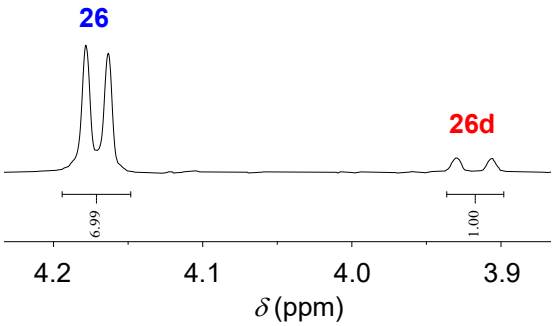

Figure S17. Diagnostic regions of crude ^{1}H NMR spectrum of the reaction mixture of **25** and **16** used to determine the diastereomeric ratio of **26** and **26d** catalyzed by **13**.

4. References

(S1) A. Molliet, S. Doninelli, L. Hong, B. Tran, M. Debas, S. Salentinig, A. F. M. Kilbinger and T. Casalini. Solvent Dependent Folding of an Amphiphilic Polyaramid. *J. Am. Chem. Soc.* **2023**, *145*, 27830-27837.

(S2) (a) M. P. Demartino and H. A. Guan, Pyridone derivatives as rearranged during transfection (RET) kinase inhibitors. Patent, WO 2016/038552 A1; (b) D. E. Welch, R. R. Baron, B. A. Burton, α, α, α-Trifluorotoluamides as Anticoccidial Agents. *J. Med. Chem.* **1969**, *12*, 299–303.

(S3) S. K. Dey and G. Das, Fluoride Selectivity Induced Transformation of Charged Anion Complexes into Unimolecular Capsule of a π-Acidic Triamide Receptor Stabilized by Strong N–H···F^- and C–H···F^- Hydrogen Bonds. *Cryst. Growth Des*. 2011, **11**, 4463–4473.

(S4) Y. Zhao, S. Benz, N. Sakai and S. Matile, *Chem. Sci*. 2015, **6**, 6219–6223.

(S5) Y. Cotelle, S. Benz, A.-J. Avestro, T. R. Ward, N. Sakai and S. Matile, *Angew. Chem. Int. Ed*. 2016, **55**, 4275–4279.

(S6) A.-B. Bornhof, A. Bauzá, A. Aster, M. Pupier, A. Frontera, E. Vauthey, N. Sakai and S. Matile, *J. Am. Chem. Soc*. 2018, **140**, 4884–4892.

(S7) (a) Y. Wang, X. Liu and L. Deng, *J. Am. Chem. Soc.,* 2006, **128**, 3928–3930; (b) X. Zhang, L. Liu, J. Lopez-Andarias, C. Wang, N. Sakai and S. Matile, *Helv. Chim. Acta*, 2018, **101**, e1700288.

(S8) L. Liu, Y. Cotelle, A.-B. Bornhof, C. Besnard, N. Sakai and S. Matile, *Angew. Chem. Int. Ed*., 2017, **56**, 13066.

(S9) (a) M. Rueping, A. Kuenkel and R. Frohlich, *Chem. Eur. J*., 2010, **16**, 4173–4176; (b) L. Liu, Y. Cotelle, J. Klehr, N. Sakai, T. R. Ward and S. Matile, *Chem. Sci.*, 2017, **8**, 3770–3774.

5. NMR Spectra

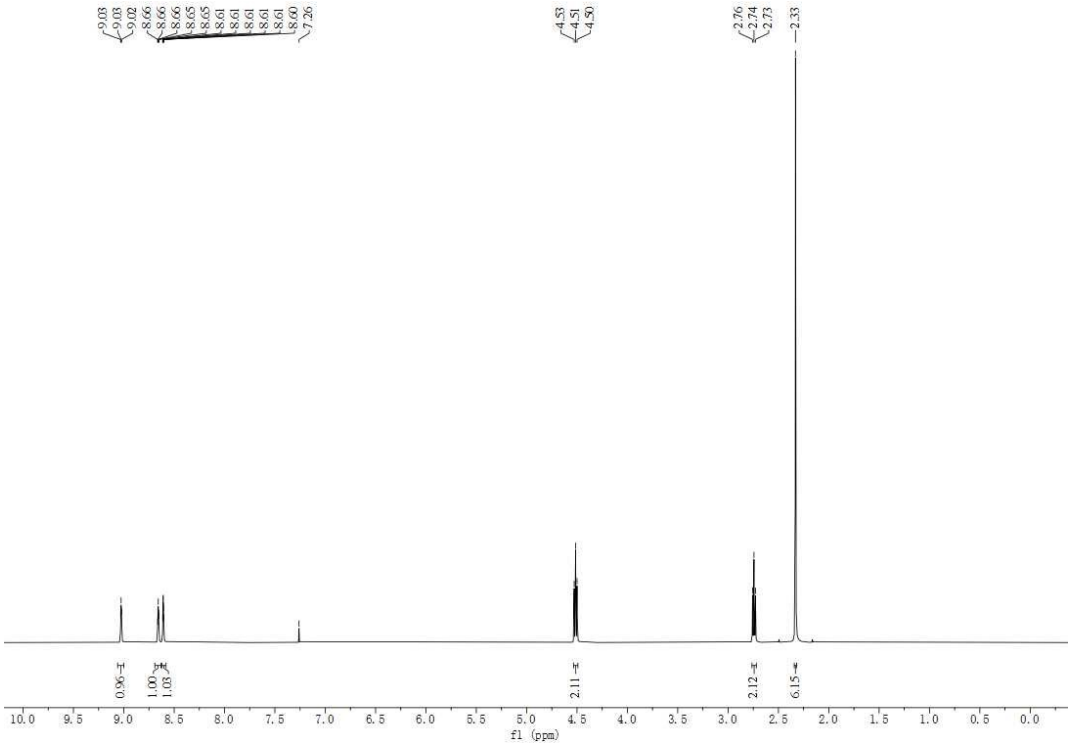

Figure S18. ^{1}H NMR spectrum of **1** in $CDCl_3$.

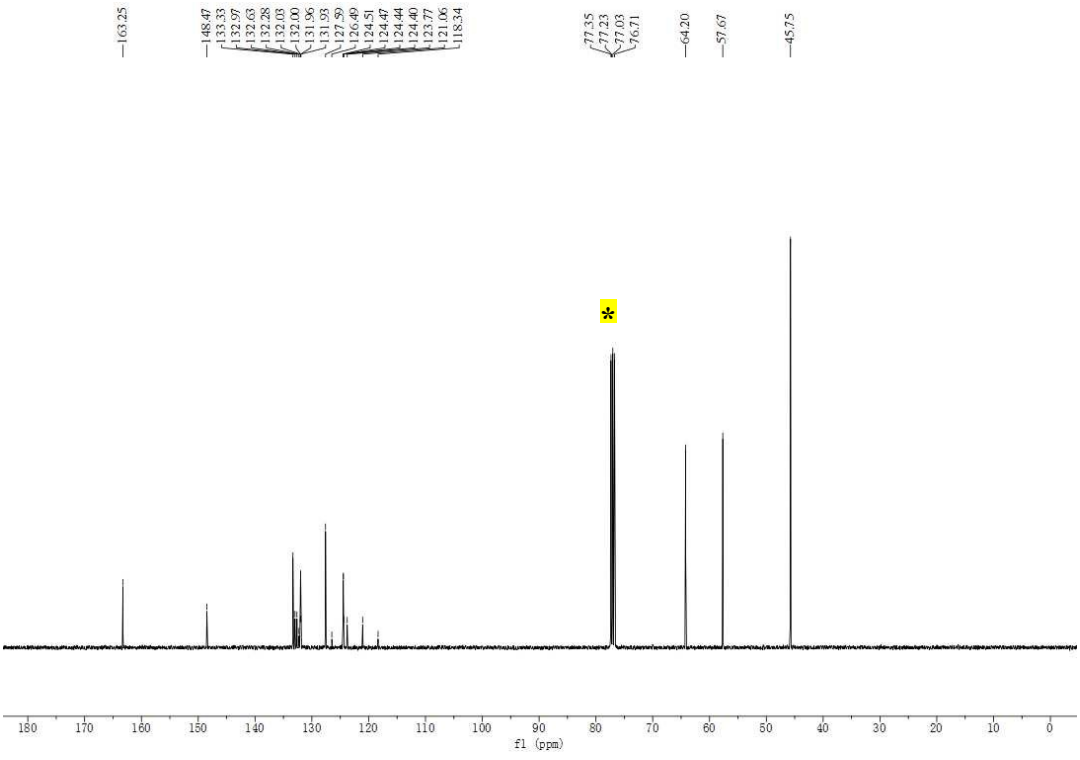

Figure S19. ^{13}C NMR spectrum of **1** in $CDCl_3$.

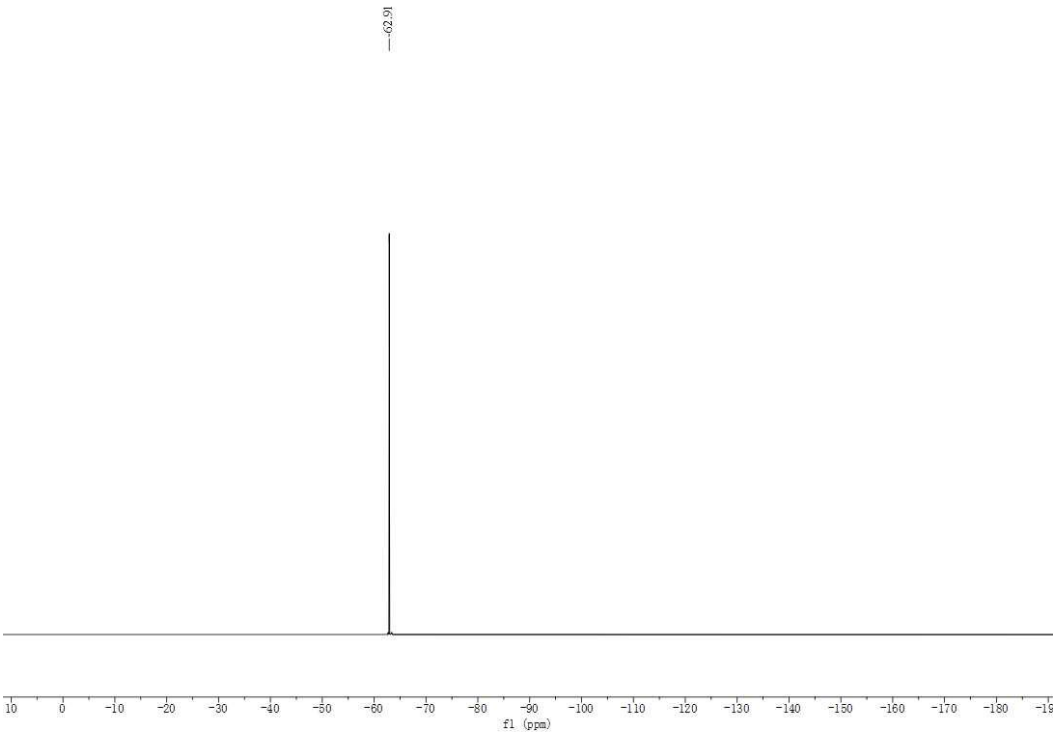

Figure S20. ^{19}F NMR spectrum of **1** in $CDCl_3$.

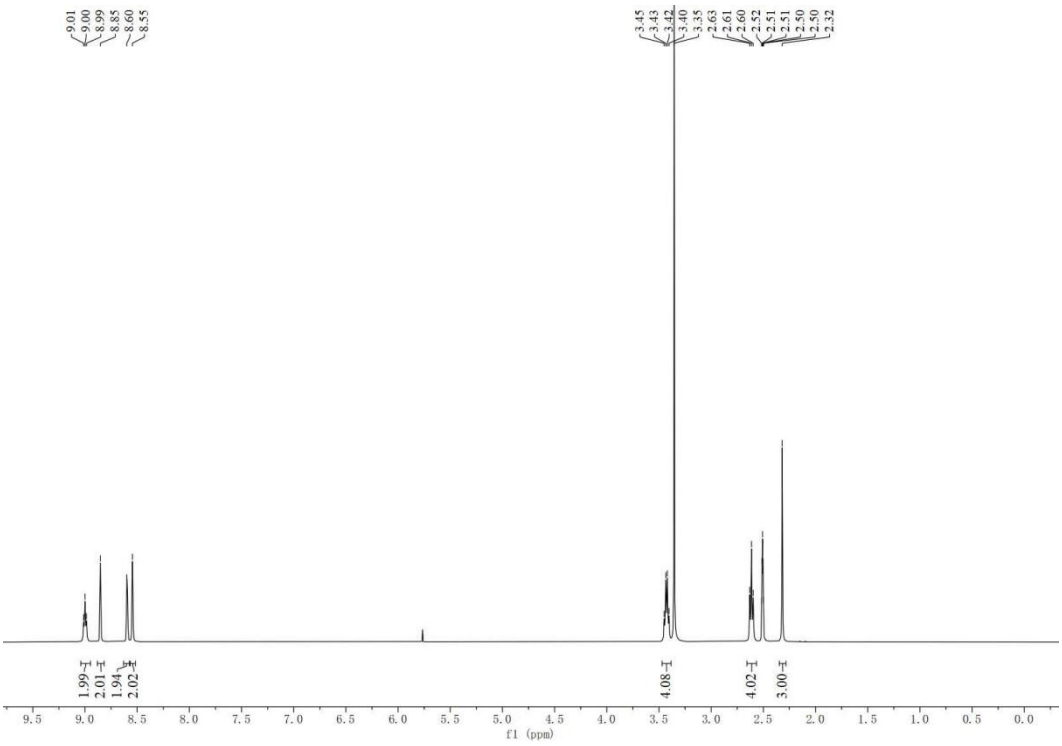

Figure S21. ^{1}H NMR spectrum of **5** in DMSO-d_6.

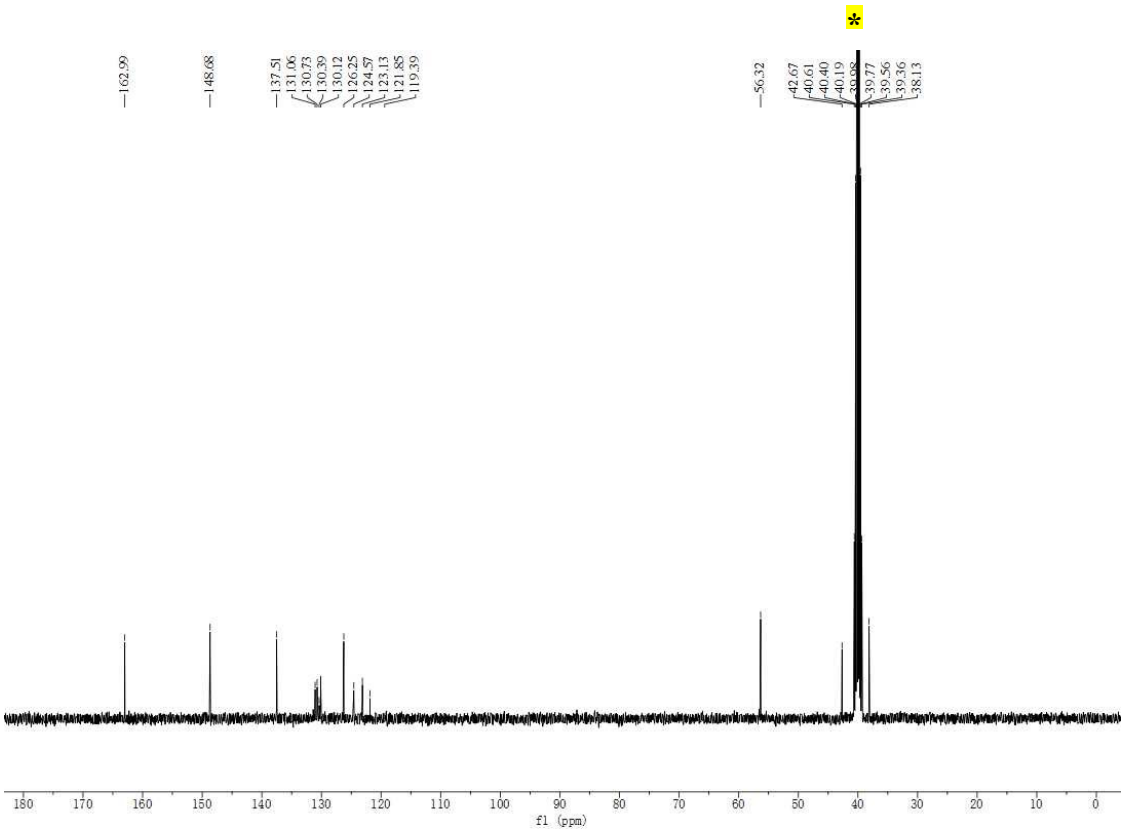

Figure S22. ^{13}C NMR spectrum of **5** in DMSO-d_6.

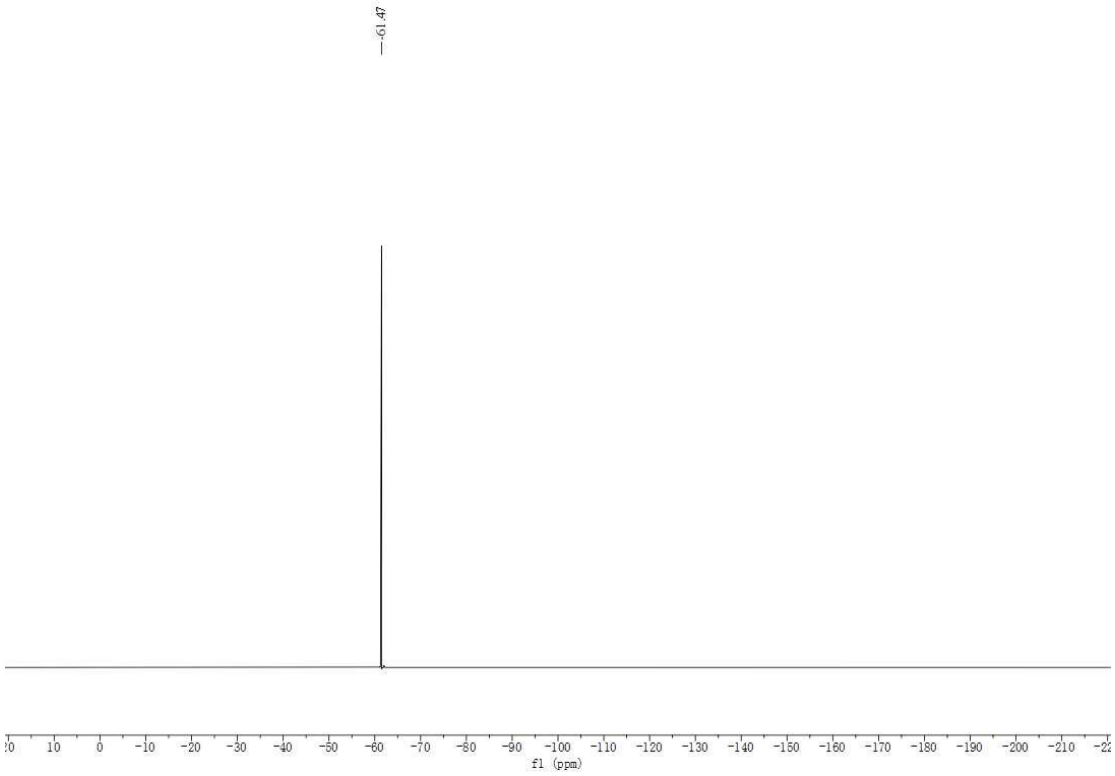

Figure S23. ^{19}F NMR spectrum of **5** in DMSO-d_6.

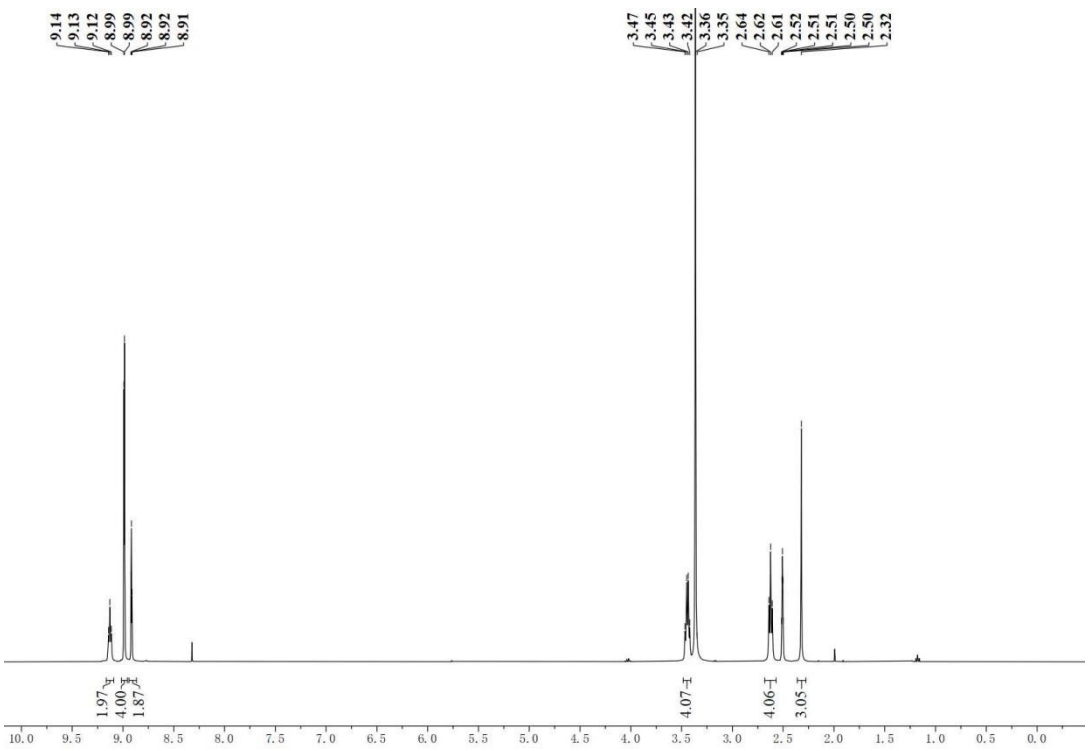

Figure S24. ^{1}H NMR spectrum of **6** in DMSO-d_6.

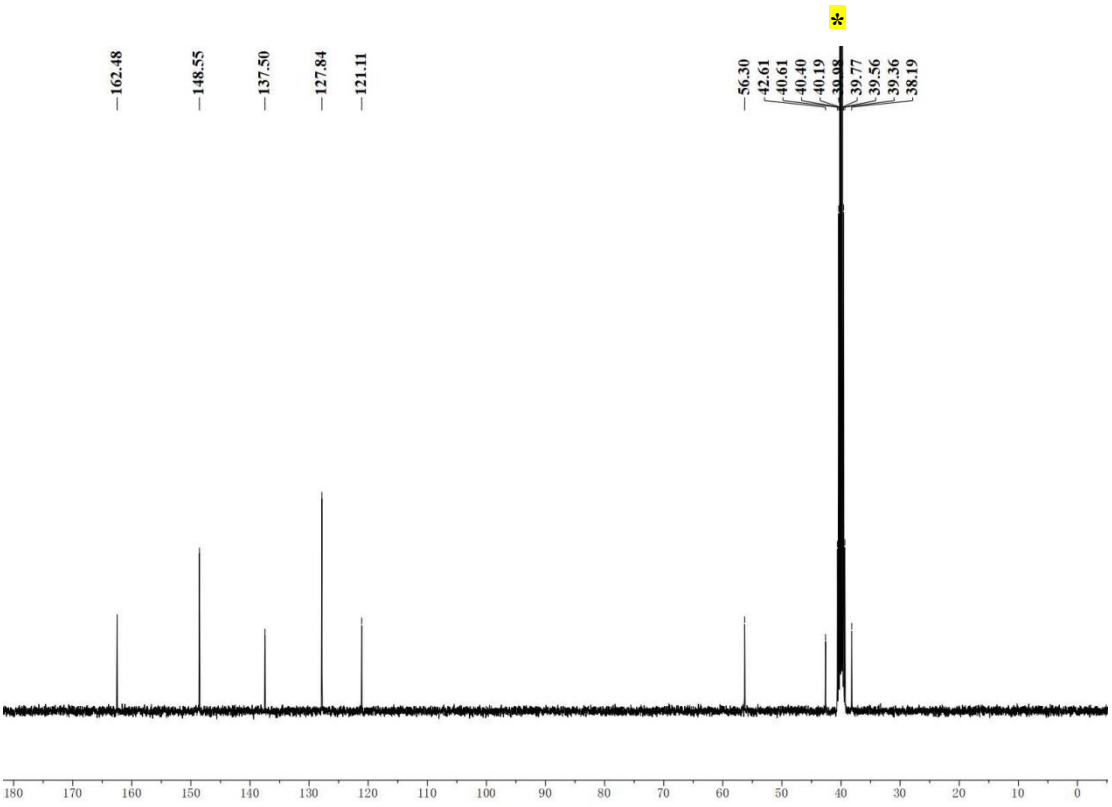

Figure S25. ^{13}C NMR spectrum of **6** in DMSO-d_6.

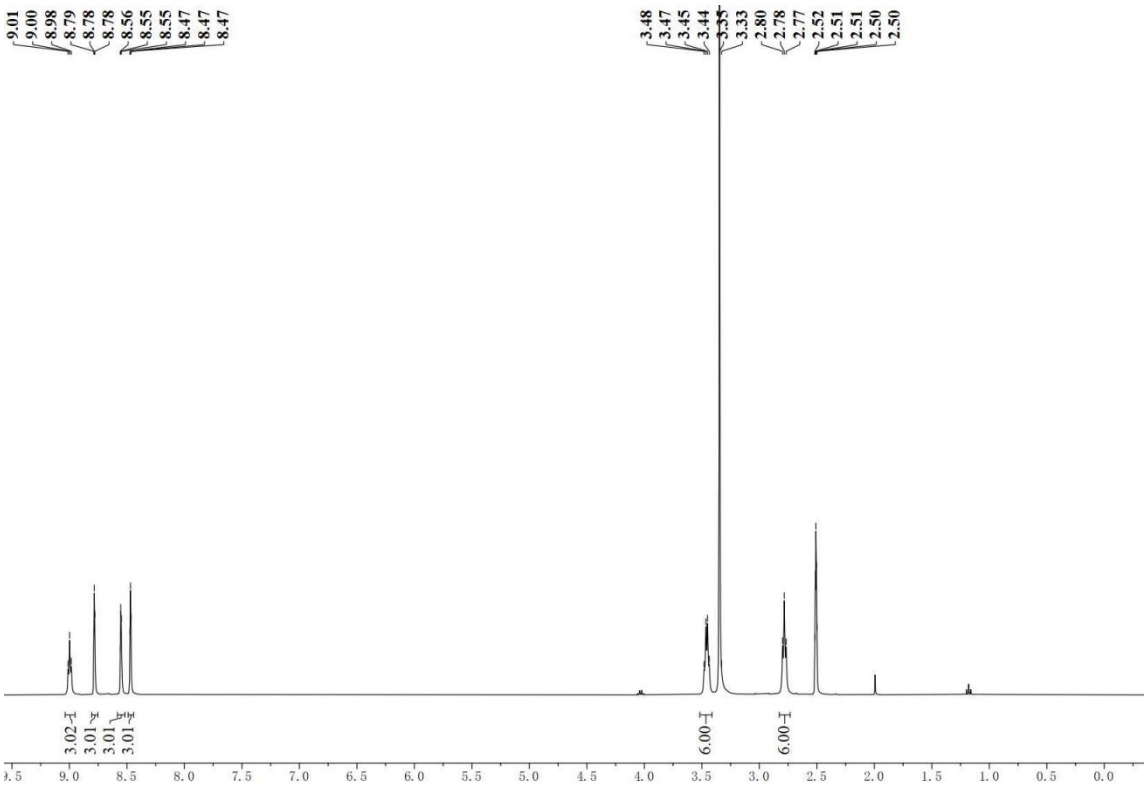

Figure S26. ^{1}H NMR spectrum of **7** in DMSO-d_6.

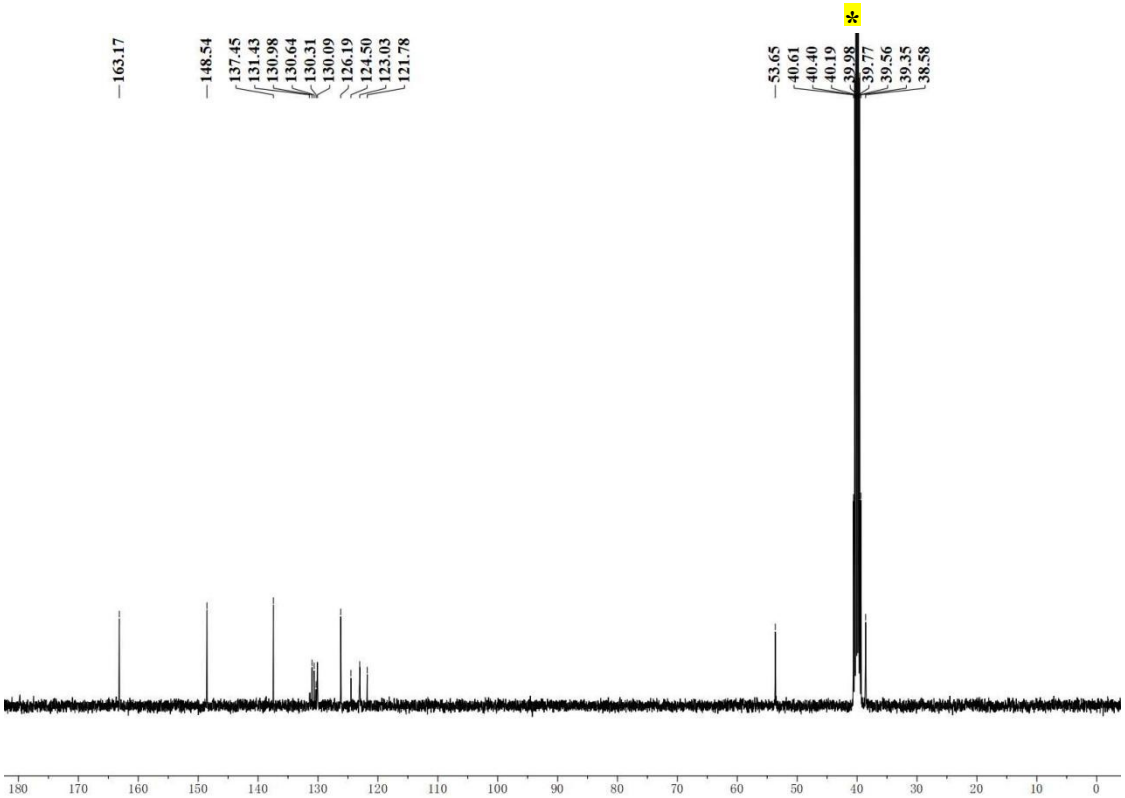

Figure S27. ^{13}C NMR spectrum of **7** in DMSO-d_6.

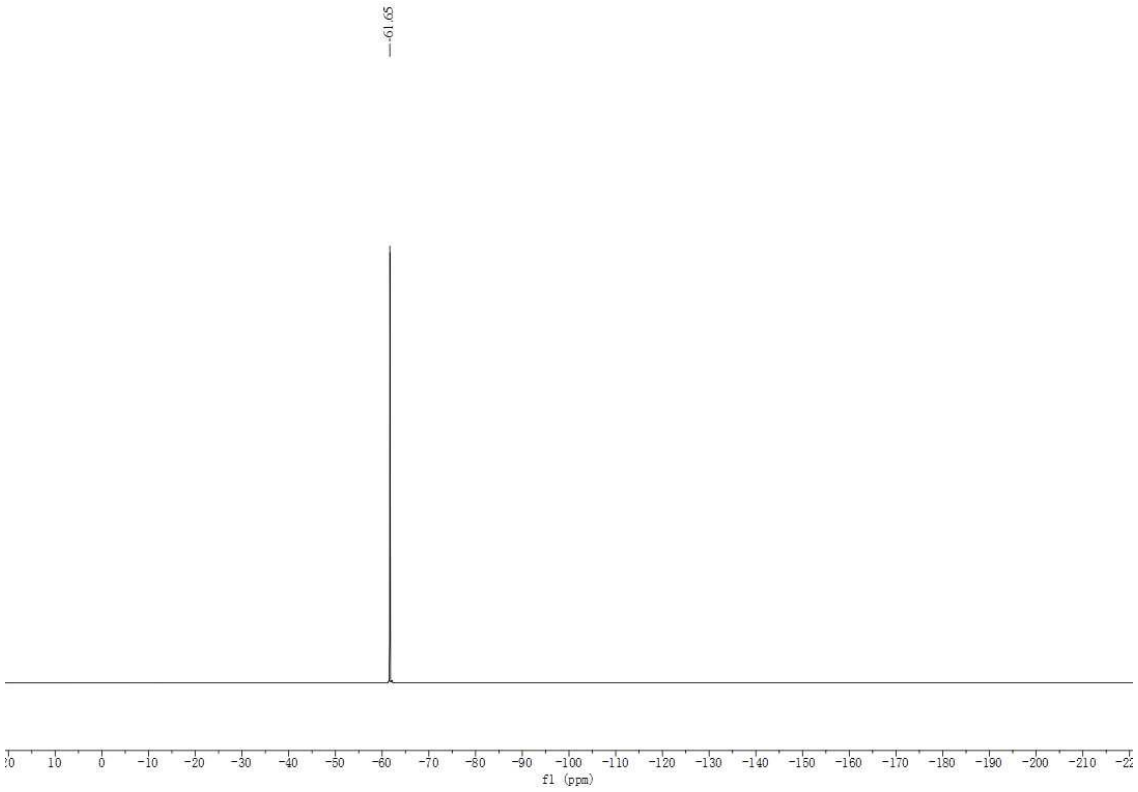

Figure S28. ^{19}F NMR spectrum of **7** in DMSO-d_6.

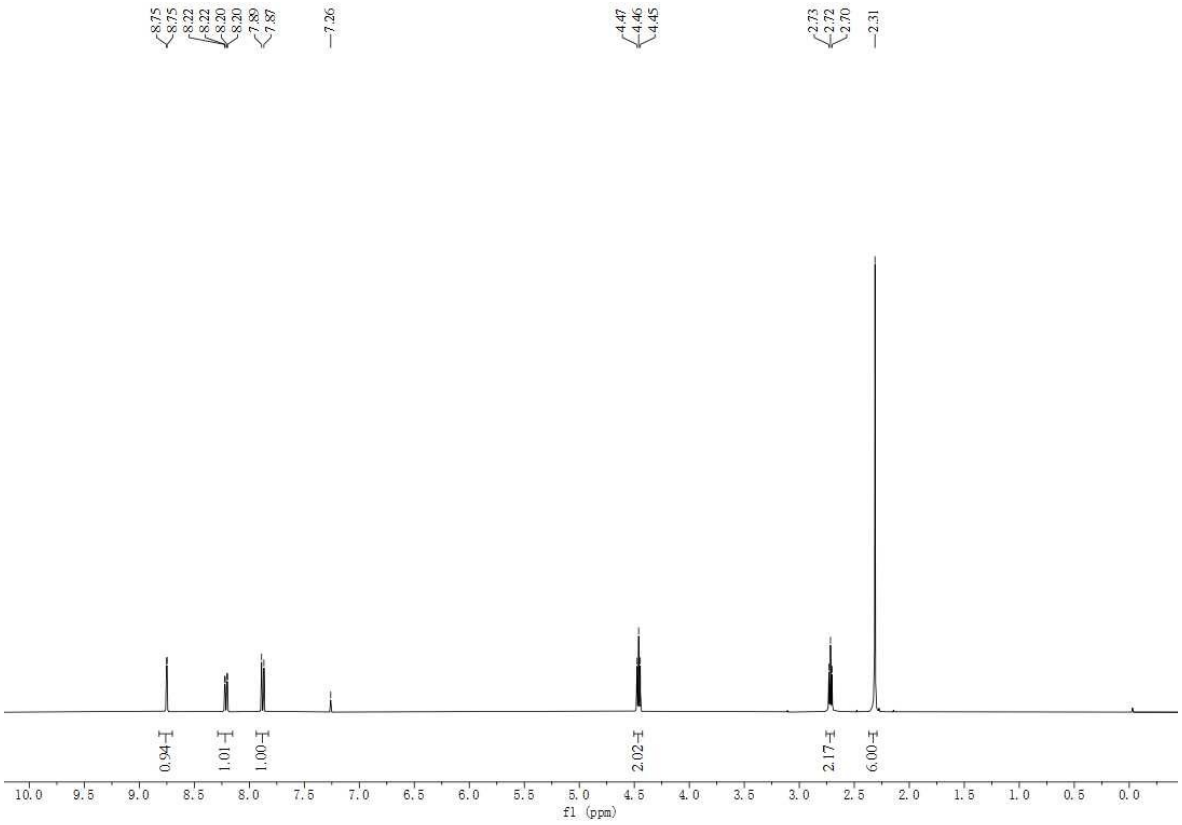

Figure S29. ^{1}H NMR spectrum of **9** in $CDCl_3$.

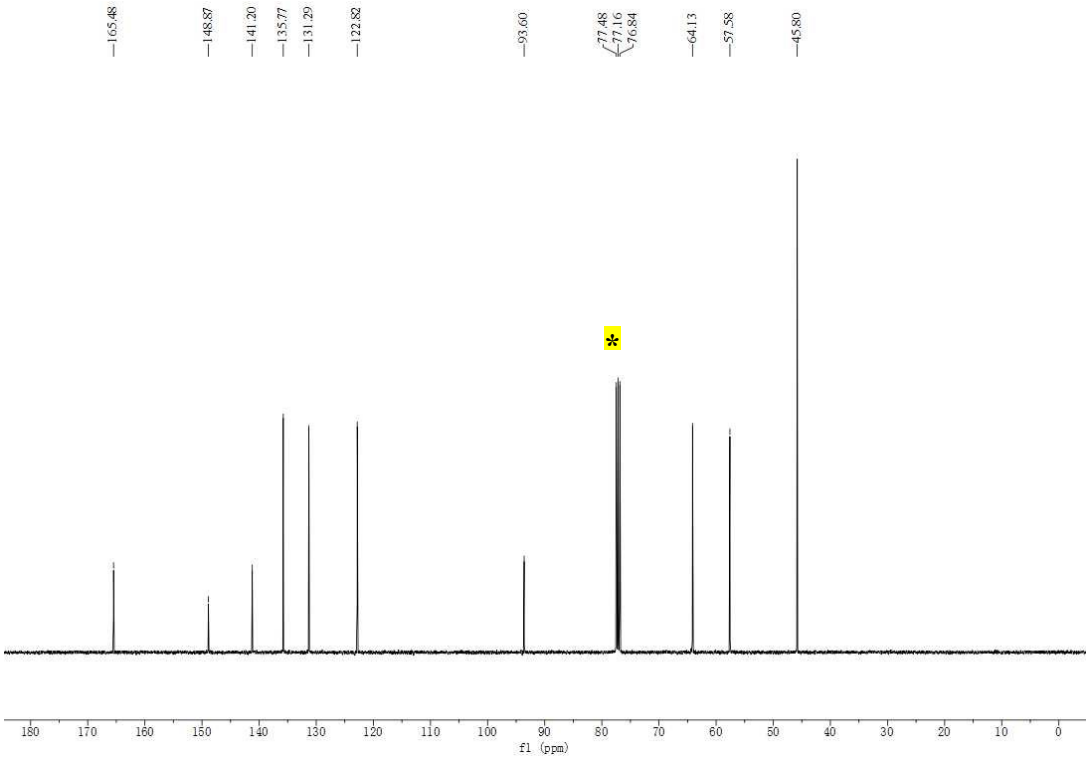

Figure S30. ^{13}C NMR spectrum of **9** in $CDCl_3$.

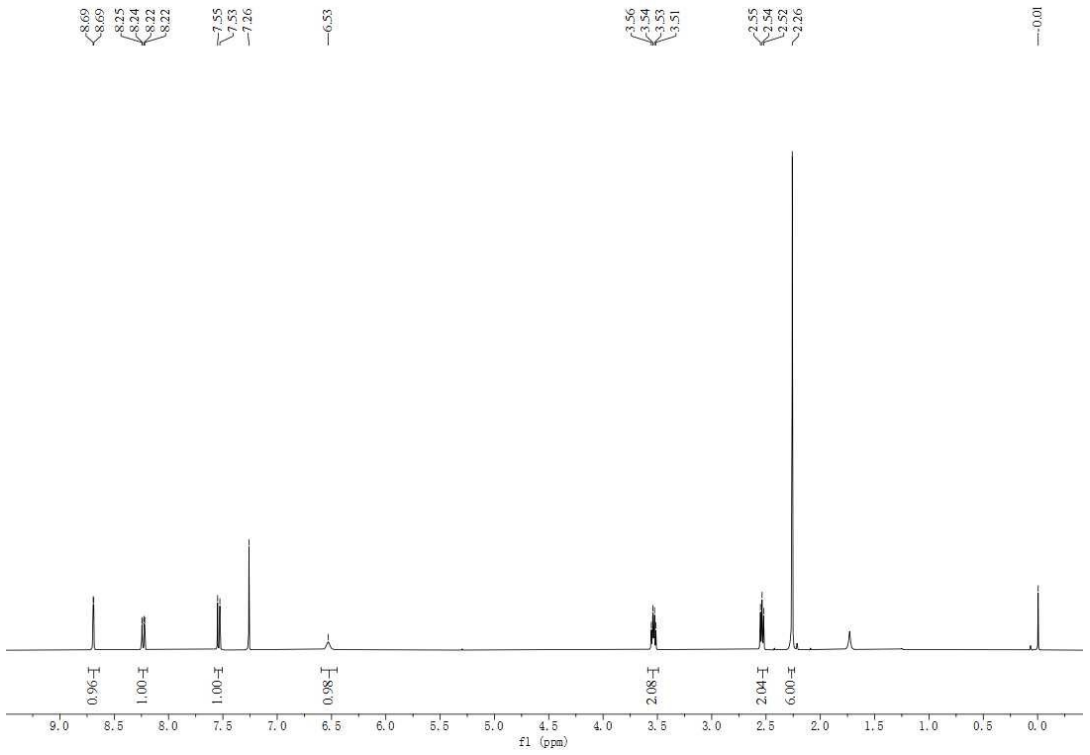

Figure S31. ^{1}H NMR spectrum of **10** in DMSO-d_6.

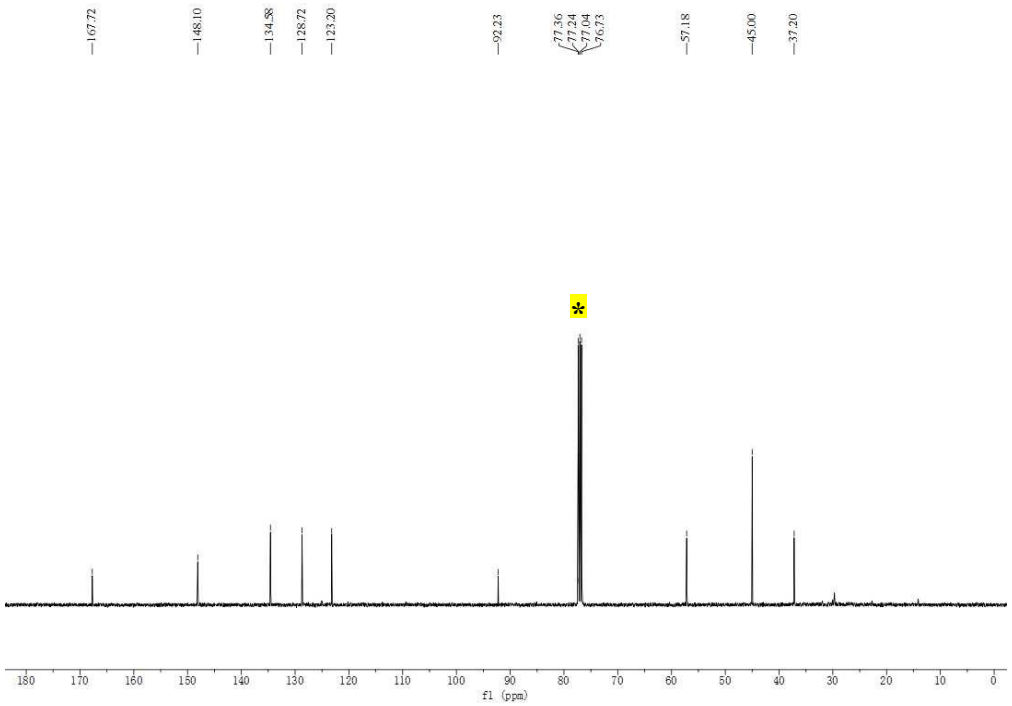

Figure S32. ^{13}C NMR spectrum of **10** in DMSO-d_6.

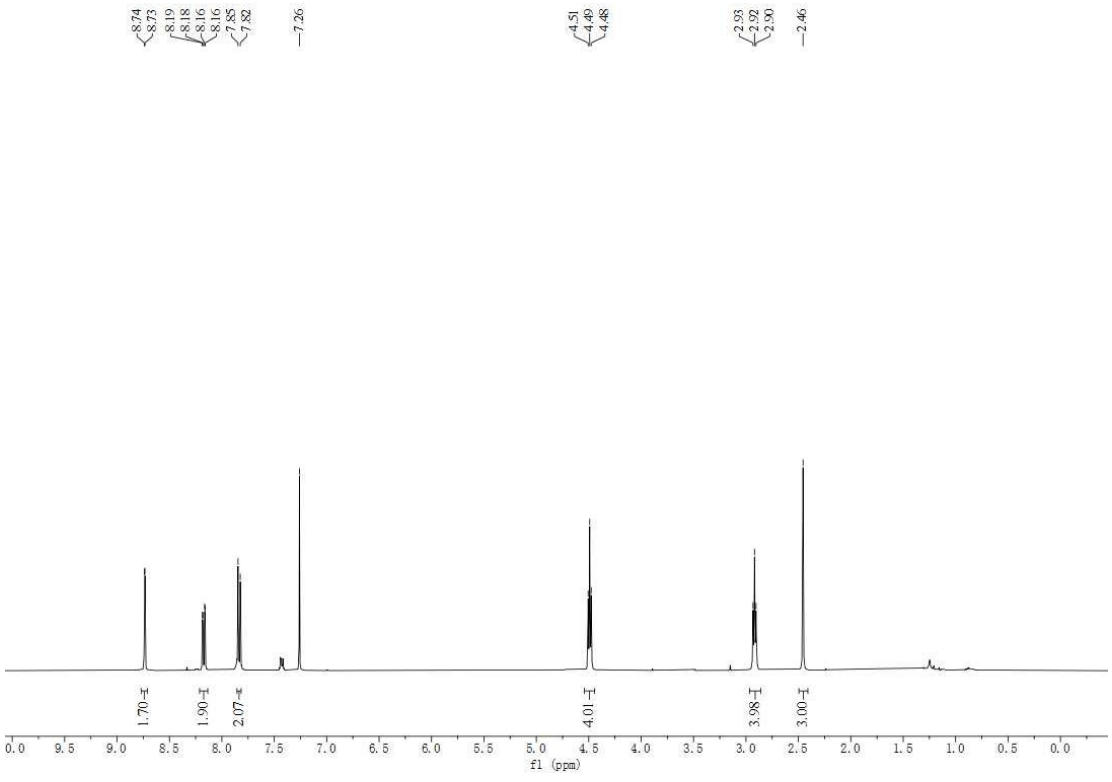

Figure S33. ^{1}H NMR spectrum of **11** in $CDCl_3$.

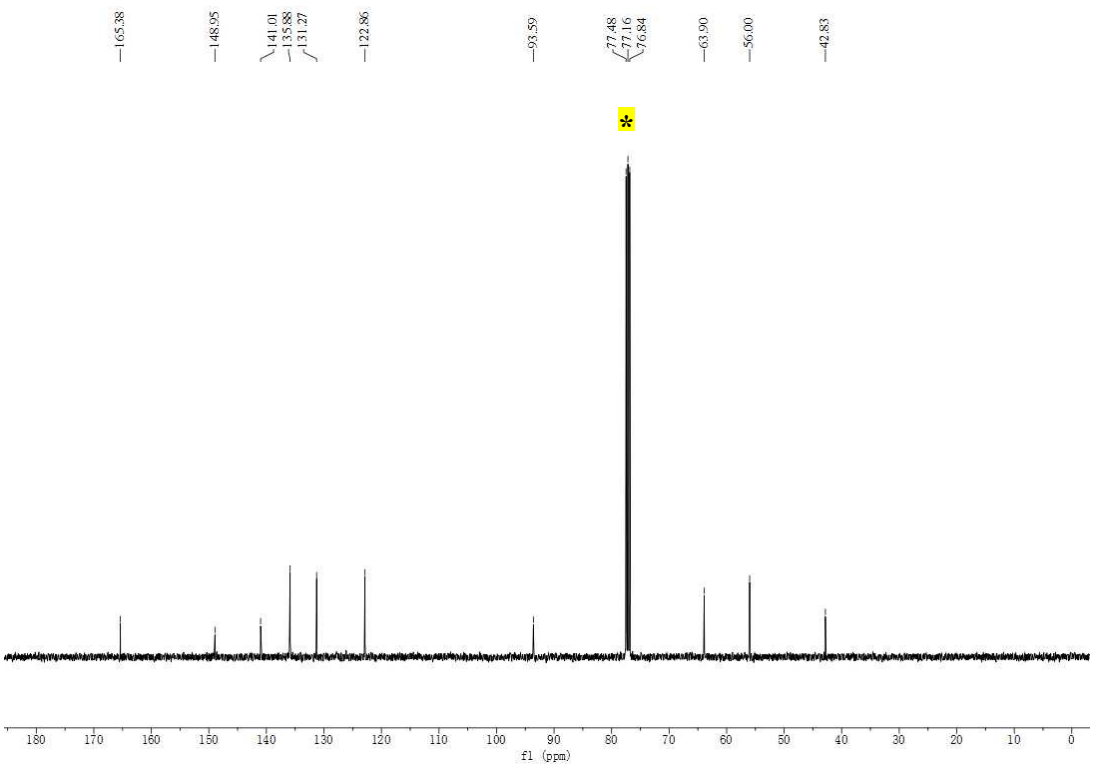

Figure S34. ^{13}C NMR spectrum of **11** in $CDCl_3$.

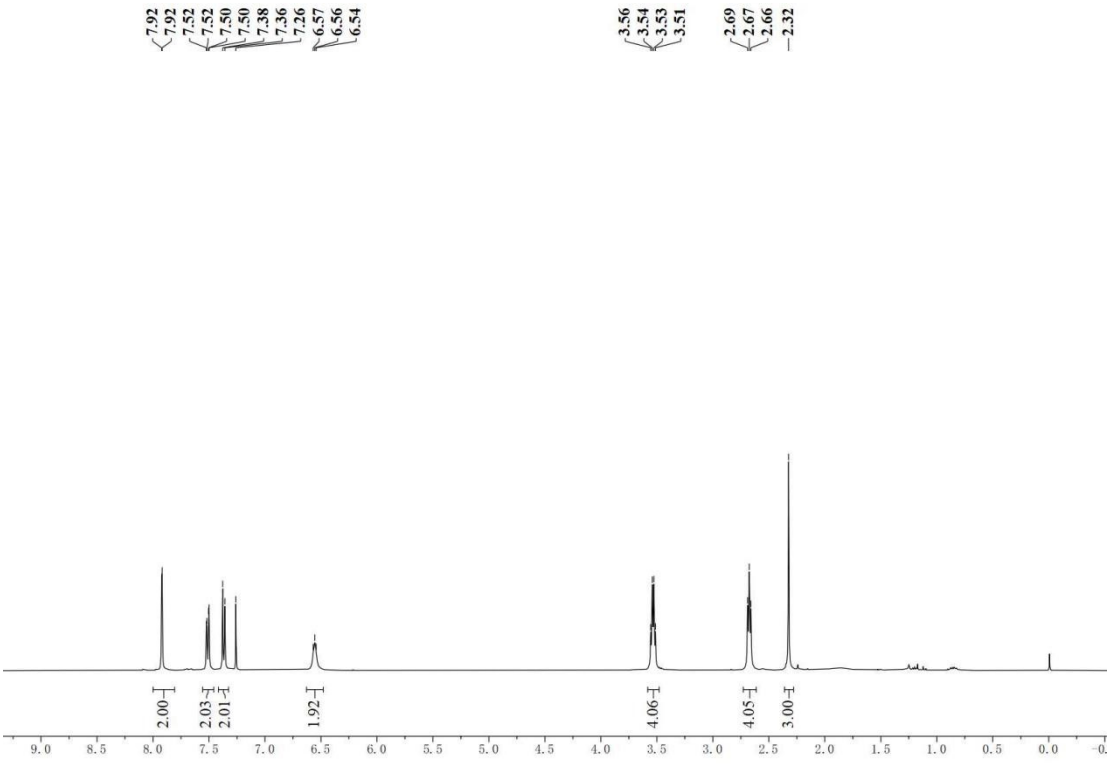

Figure S35. ^{1}H NMR spectrum of **12** in $CDCl_3$.

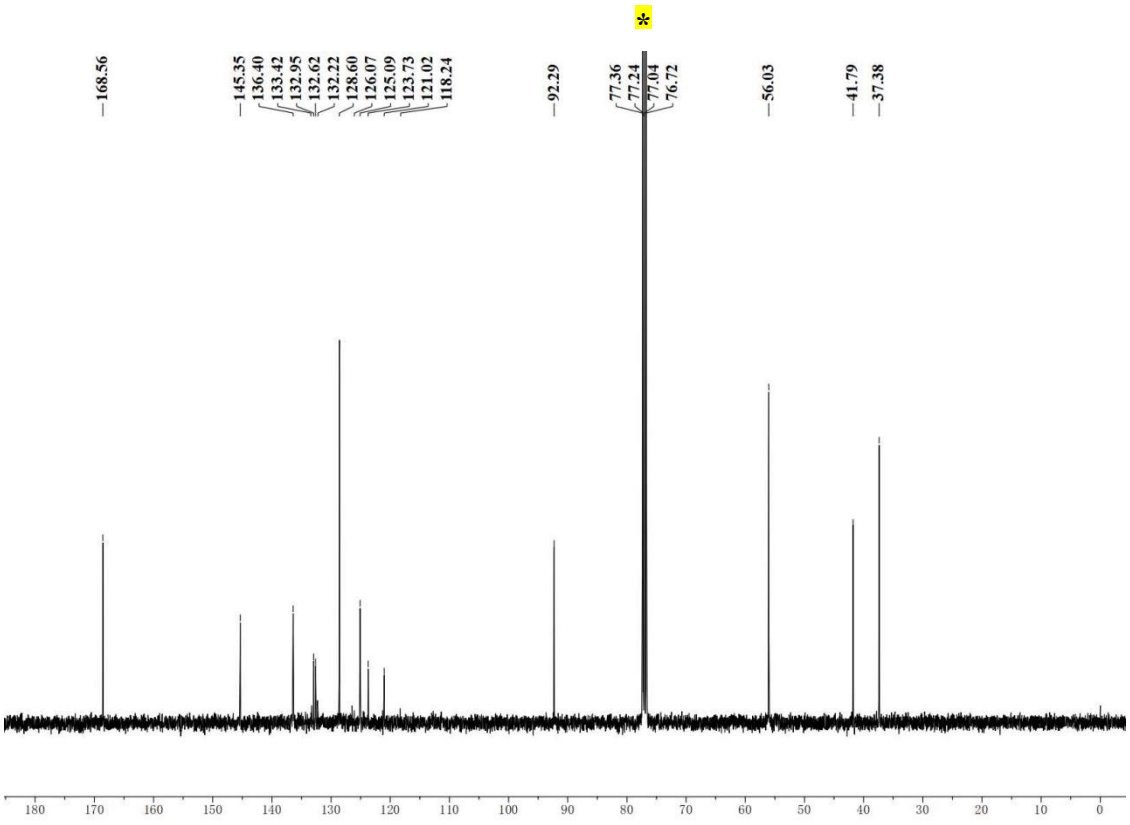

Figure S36. ^{13}C NMR spectrum of **12** in $CDCl_3$.

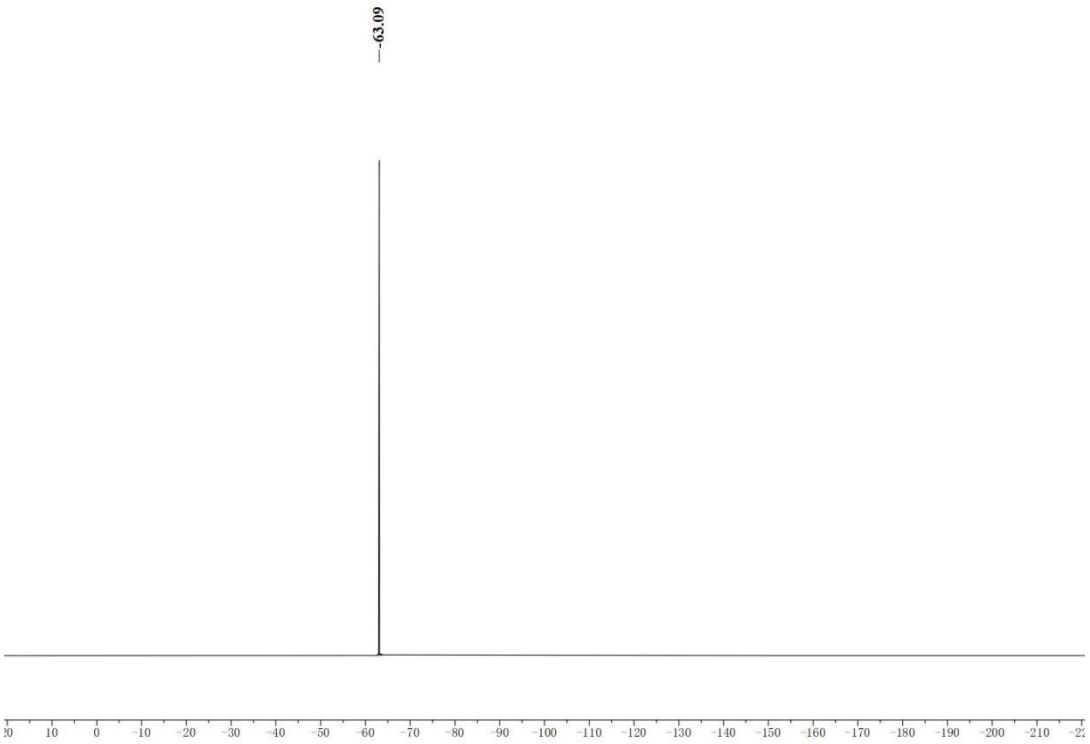

Figure S37. ^{19}F NMR spectrum of **12** in $CDCl_3$.

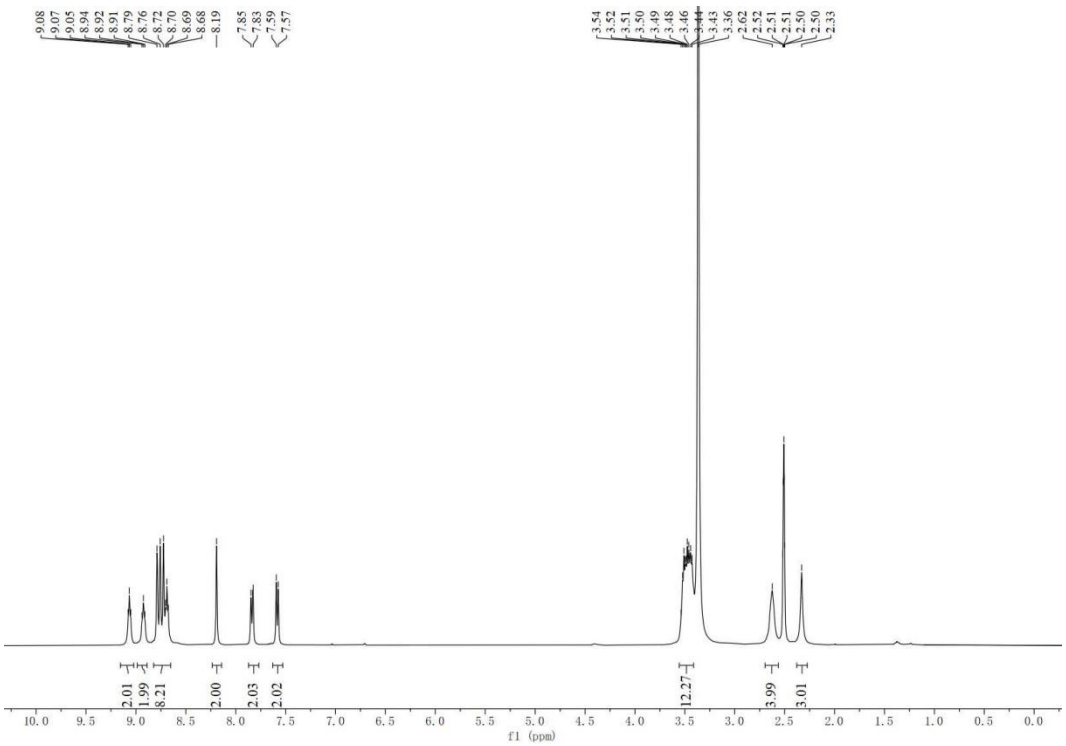

Figure S38. ^{1}H NMR spectrum of **13** in DMSO-d_6.

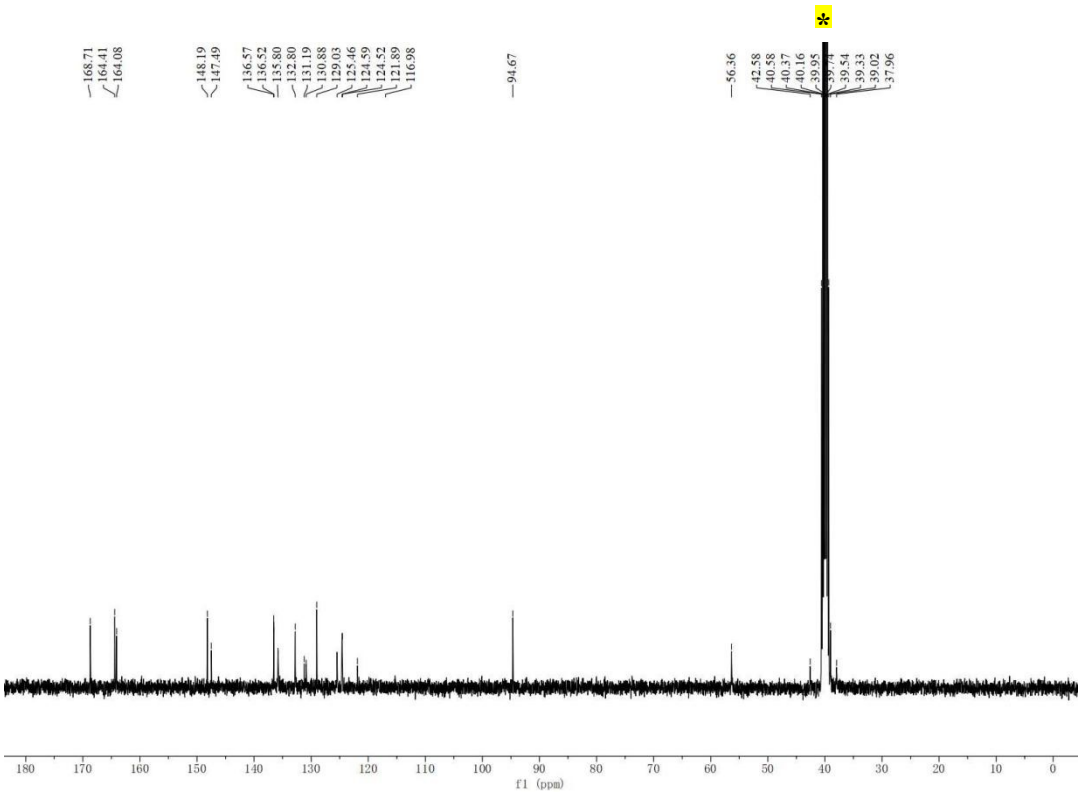

Figure S39. ^{13}C NMR spectrum of **13** in DMSO-d_6.

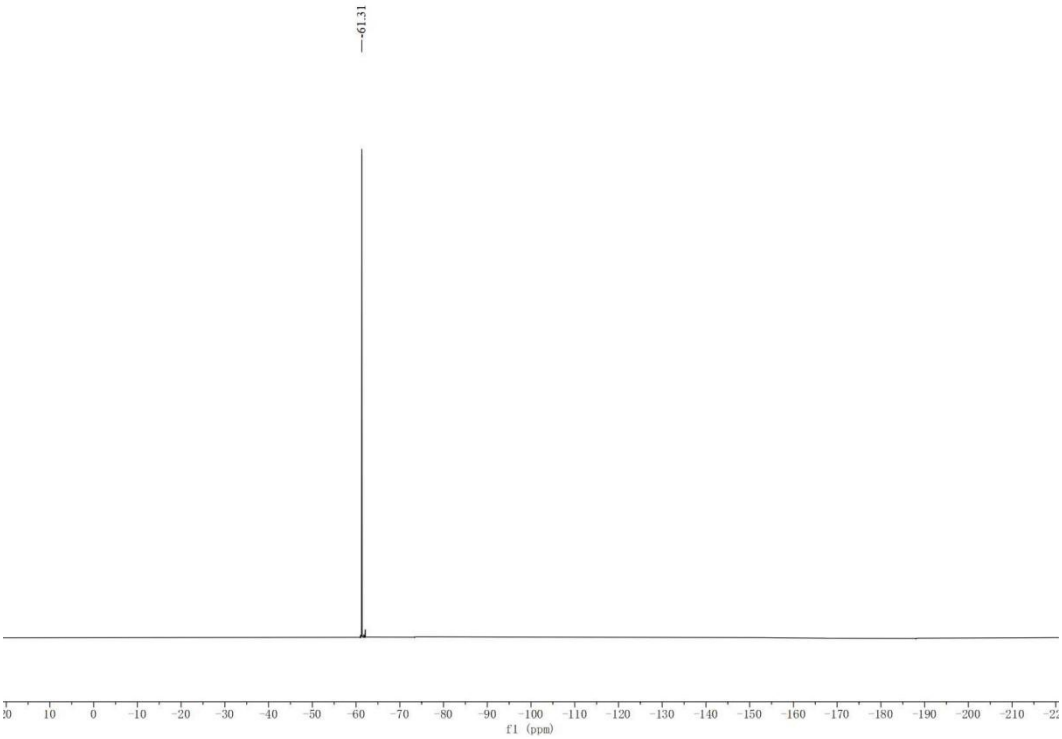

Figure S40. ^{19}F NMR spectrum of **13** in DMSO-d_6.

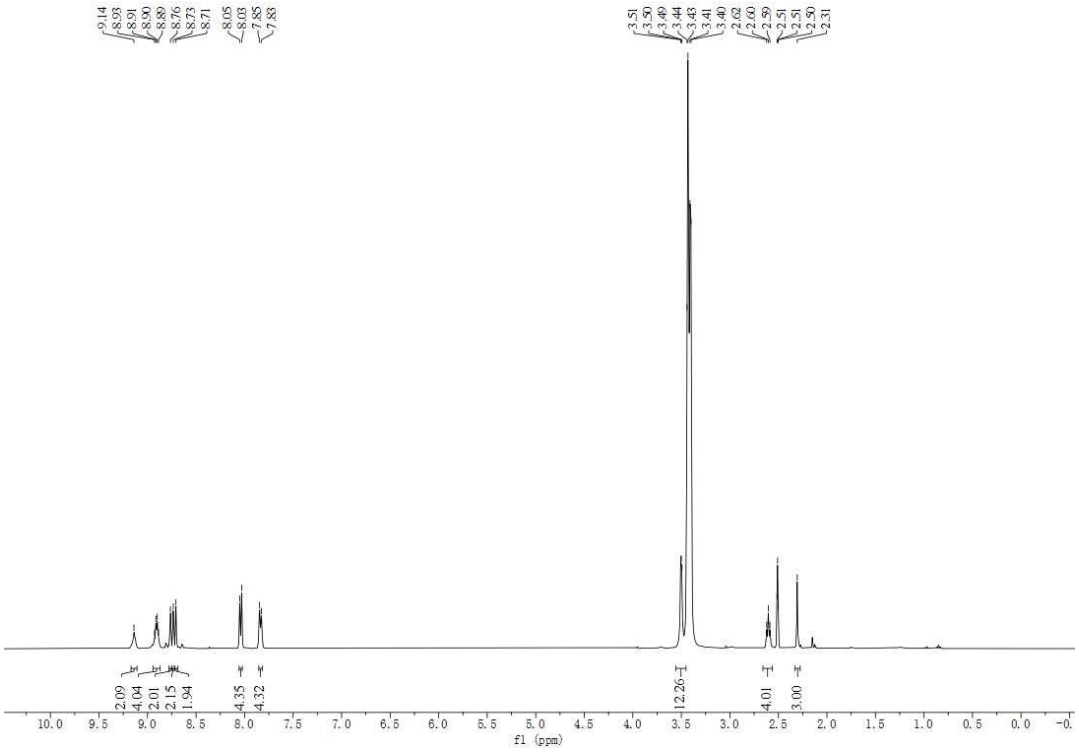

Figure S41. ^{1}H NMR spectrum of **14** in DMSO-d_6.

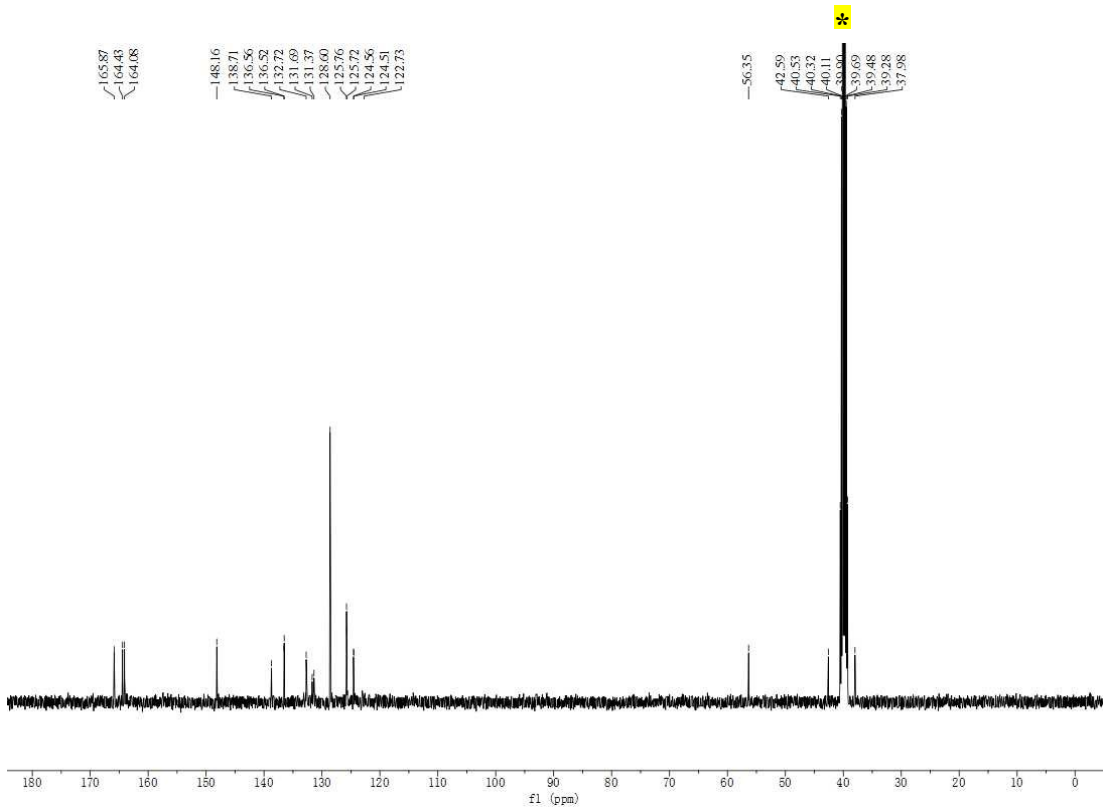

Figure S42. ^{13}C NMR spectrum of **14** in DMSO-d_6.

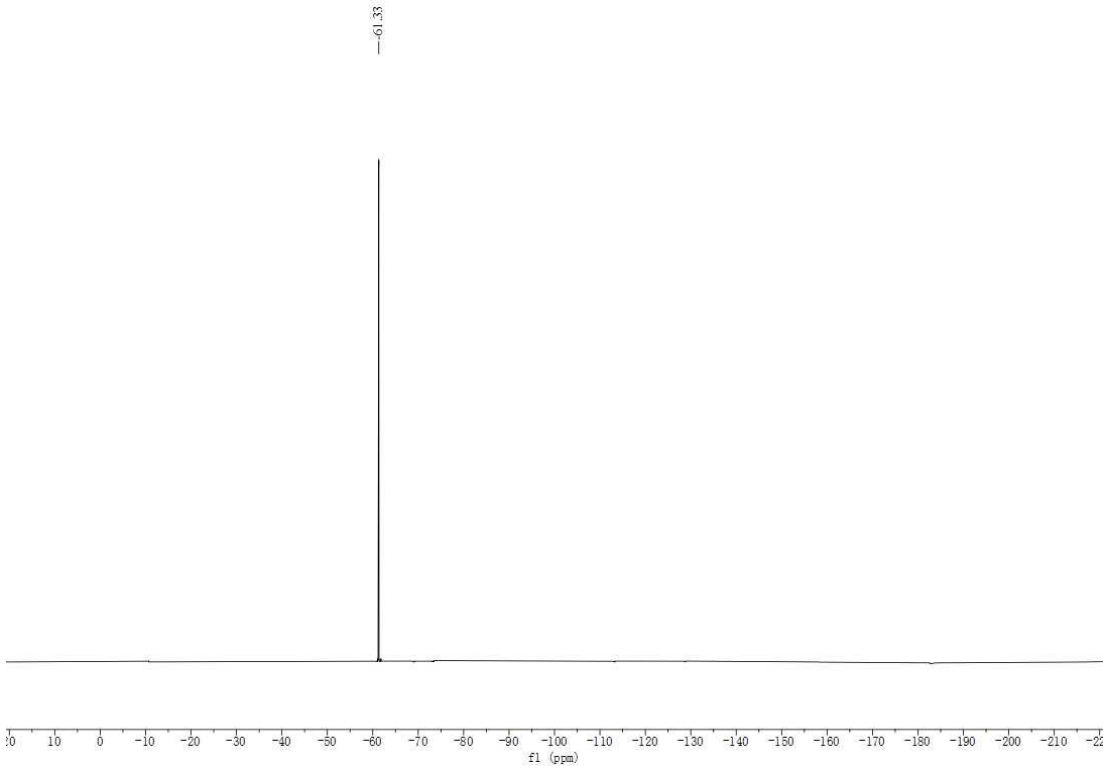

Figure S43. ^{19}F NMR spectrum of **14** in DMSO-d_6.